

RESEARCH ARTICLE

Contrasting Effects of Historical Sea Level Rise and Contemporary Ocean Currents on Regional Gene Flow of *Rhizophora racemosa* in Eastern Atlantic Mangroves

Magdalene N. Ngeve^{1*}, Tom Van der Stocken¹, Dimitris Menemenlis², Nico Koedam¹, Ludwig Triest¹

1 Laboratory of Plant Biology and Nature Management (APNA), Department of Biology, Vrije Universiteit Brussel (VUB), Pleinlaan 2, B-1050, Brussels, Belgium, **2** Earth Sciences Division, Jet Propulsion Laboratory, California Institute of Technology, Pasadena, California, United States of America

* ngevem@yahoo.com; magdale@vub.ac.be



OPEN ACCESS

Citation: Ngeve MN, Van der Stocken T, Menemenlis D, Koedam N, Triest L (2016) Contrasting Effects of Historical Sea Level Rise and Contemporary Ocean Currents on Regional Gene Flow of *Rhizophora racemosa* in Eastern Atlantic Mangroves. PLoS ONE 11(3): e0150950. doi:10.1371/journal.pone.0150950

Editor: Shing Yip Lee, Griffith University, AUSTRALIA

Received: November 12, 2015

Accepted: February 22, 2016

Published: March 10, 2016

Copyright: © 2016 Ngeve et al. This is an open access article distributed under the terms of the [Creative Commons Attribution License](https://creativecommons.org/licenses/by/4.0/), which permits unrestricted use, distribution, and reproduction in any medium, provided the original author and source are credited.

Data Availability Statement: All relevant data are within the paper and its Supporting Information files.

Funding: This study was financed by the Vrije Universiteit Brussel—International Relations and Mobility Office (VUB—IRMO) Doctoral Scholarship awarded to M.N. Ngeve. The Doctoral School NSE of the VUB also awarded a travel grant (NSE-TG-2013-82) to M.N. Ngeve. The BAS 42 funding of the VUB also supported the laboratory analyses of this study. The funders had no role in study design, data collection and analysis, decision to publish, or preparation of the manuscript.

Abstract

Mangroves are seafaring taxa through their hydrochorous propagules that have the potential to disperse over long distances. Therefore, investigating their patterns of gene flow provides insights on the processes involved in the spatial genetic structuring of populations. The coastline of Cameroon has a particular geomorphological history and coastal hydrology with complex contemporary patterns of ocean currents, which we hypothesize to have effects on the spatial configuration and composition of present-day mangroves within its spans. A total of 982 trees were sampled from 33 transects (11 sites) in 4 estuaries. Using 11 polymorphic SSR markers, we investigated genetic diversity and structure of *Rhizophora racemosa*, a widespread species in the region. Genetic diversity was low to moderate and genetic differentiation between nearly all population pairs was significant. Bayesian clustering analysis, PCoA, estimates of contemporary migration rates and identification of barriers to gene flow were used and complemented with estimated dispersal trajectories of hourly released virtual propagules, using high-resolution surface current from a mesoscale and tide-resolving ocean simulation. These indicate that the Cameroon Volcanic Line (CVL) is not a present-day barrier to gene flow. Rather, the Inter-Bioko-Cameroon (IBC) corridor, formed due to sea level rise, allows for connectivity between two mangrove areas that were isolated during glacial times by the CVL. Genetic data and numerical ocean simulations indicated that an oceanic convergence zone near the Cameroon Estuary complex (CEC) presents a strong barrier to gene flow, resulting in genetic discontinuities between the mangrove areas on either side. This convergence did not result in higher genetic diversity at the CEC as we had hypothesized. In conclusion, the genetic structure of *Rhizophora racemosa* is maintained by the contrasting effects of the contemporary oceanic convergence and historical climate change-induced sea level rise.

Competing Interests: The authors have declared that no competing interests exist.

Introduction

The potential effects of climate change on coastal ecosystems have received heightened attention recently [1]. Mangrove ecosystems are considered resilient under changing environmental conditions [2–5], with potential expansion in some areas [1, 5]. Landward expansion, for example, has been reported in localities where overall accretion keeps pace with relative sea level rise (SLR) *i.e.*, accretionary surplus [1, 2, 6, 7], while pole-ward (latitudinal) expansion may occur in response to rising temperatures, *i.e.*, higher average winter temperatures [2, 8–10]. SLR may also favor landward mangrove expansion by decreasing subsidence, increasing saline intrusion, and changing the ground water level in coastal areas, thereby allowing mangroves to thrive over other vegetation [1]. Besides SLR, changing climatic conditions also include changes in the frequency and intensity of extreme meteorological events such as tropical cyclones [11]. Although solid evidence is yet missing, such meteorological trends may favor biogeographic range expansion through fostering long distance dispersal (LDD) by increasing the vector (ocean surface current) seed load, vector displacement velocity, and seed passage time [12]. Dispersal processes over oceans have shaped ranges of mangroves and the genetic structure of populations throughout the species' existence, but evidence is needed as to the timescale and settings which define the outcome that are actually observed. Understanding dispersal processes of the past may give insight to species responses to future climate change.

Mangrove ecosystems occur along coastal areas in the (sub)-tropics, approximately between 30° N and 30° S. Their socio-economic and ecological importance has been widely recognized [13–18], rendering them an integral part of the daily lives of many coastal communities. The importance of these ecosystems, however, is not restricted to their biogeographical extent. Despite occupying only 0.7% of the tropical forest area, mangrove degradation may contribute to more than 10% of global carbon emissions due to deforestation [19]. Nevertheless, global mangrove stocks have decreased more than 40% over the last 50 years, with a continuing yearly decline of 2% [20]. By the year 2000, global mangrove cover was estimated to be 137760 km² [21]. Fossil evidence indicates that mangroves once occupied a broader geographical range than they do today [22–24] due to spatial changes in favorable temperatures. It has been hypothesized that cold temperature, in interaction with aridity, are the delimiting factors to mangrove range expansions [25–27]. Climatic oscillations of the past have also been characterized by successive range expansions and contractions for many mangrove species; range expansions after the Last Glacial Maximum (LGM) have been reported for many Neotropical species [25, 27–29]. The present distribution of mangroves is shaped by (1) suitable intertidal habitats, (2) the potential of propagules to reach these locations within their viable periods [30, 31], and (3) various thresholds to establishment [6]. The hydrochorous propagules of *Rhizophora* can remain viable and afloat for more than 3 months [32], providing a sufficiently long time window for potential LDD and the colonization of new favorable habitats. Nevertheless, multiple barriers may hamper a species from colonizing its full potential niche (*sensu* Randin *et al.* [33]), for example unfavorable ocean currents, closed estuaries, arid [34] or hard rock coastlines, and the physical disturbance by tidal inundation and wave-induced sediment dynamics [31, 35].

These factors, in addition to local pollen flow, determine the overall genetic structure as they control the exchange and fluxes of alleles between nearby and remote populations. Absence of or limited gene flow can result from vicariance [36–38], as well as distance-related dispersal limitation, where genetic differentiation shows a linear relationship with geographical distance between populations [39]. Orsini *et al.* [40] postulated that isolation of natural populations could indeed be due to either (1) distance-related dispersal limitation (Isolation by Distance; IBD), or (2) adaptation where selection pressure drives local adaptation, thereby

reducing establishment success of non-adapted immigrants (Isolation by Adaptation; IBA). Also, (3) local adaptation combined with the numerical advantage (density-dependence) of first colonists (founder effect) may contribute to a strong priority effect of residents over immigrants, thereby creating isolation by colonization (IBC) [40, 41]. However, the source of colonizers, which could either follow a migrant pool model, where colonizers originate from a pool of different but still highly connected demes (thus resulting in low differentiation despite multiple sources), or a propagule pool model, where colonizers come from a pool of already differentiated origin population (thus resulting in high differentiation) [42], is also of great significance. The use of IBD models for explaining spatial genetic differentiation among populations, dominate literature [43], irrespective of the frequent observation of dissociation between genetic differentiation and geographical distance in marine systems [44] and the erroneous assumptions associated with the use of IBD models. IBD analysis generally assumes spatial homogeneity and/or theoretically unjustified distance metrics, although landscapes are naturally heterogeneous [45]. McRae [45] proposed the use of isolation by resistance model (IBR) which takes into account landscape heterogeneity. Information on barriers to gene flow, such as ocean currents, is used to define a resistance surface, predict spatial genetic structure of populations, and to explain deviations from the widely applied IBD model [44].

In mangroves, high levels of gene flow ($F_{st} < 0.2$, $N_m > 1$) along the same stretch of coastline have been reported by several authors [46–48], likely as a result of range expansion after the LGM (28). However, genetic structure at distance classes < 1000 km in the Atlantic East Pacific (AEP) suggests high levels of short distance dispersal (SDD) (and therefore low levels of long distance dispersal), at least for *Avicennia* spp. [28, 49]. Generally, broad-ranged seafaring species exist as patchy subpopulations separated by weak barriers [50]. Several barriers to gene flow among mangrove populations have been identified worldwide, resulting in patterns of genetic discontinuities. Land barriers like the Central American Isthmus, the Malay Peninsula and the Indonesian archipelago [37, 38, 51], as well as cold currents [28] and oceanic barriers, even at spatially proximate populations [28, 52, 53] have been well established. Despite the importance of such insight in explaining and understanding the genetic structure of mangrove populations across vast expanses of ocean or along coastlines at local, regional and continental scales, information on the underlying drivers that shape the genetic structure of mangroves along the East-Atlantic coast is missing.

In this study, we assess the genetic diversity and structure of *Rhizophora racemosa* G. Mey. populations from 4 estuaries along the coast of Cameroon. It is likely that the historical and current barriers, as well as the recent dispersal corridor on this coastline (see “[Study area](#)” below) may explain, at least partly, the configuration and composition of present-day mangrove forest in this area (*ca.* 400 km, which makes up *ca.* 6% of the mangrove coastline of the East Atlantic). The spatial configuration of mangroves along this coastline relative to past and present-day oceanographic and geomorphologic characteristics provides an interesting case to test the hypotheses that: (1) the historical barrier of the Cameroon Volcanic Line (CVL) (at the Bioko-mainland connection) has affected gene flow such that populations on either side of this barrier are isolated; (2) the presence of an ocean current convergence zone represents an important oceanic barrier to gene flow causing genetic discontinuity between populations on both sides of its frontal zone; and (3) the ocean current convergence zone results in higher genetic diversity of mangroves of the Cameroon Estuary complex (CEC) than among mangrove populations on either side of this convergence zone, due to input of propagules from areas north and south of it.

Materials and Methods

Ethics Statement

Permission to collect samples in the Campo Ma'an National Park and the Douala-Edea Reserve at Mouanko was obtained from the Ministry of Forestry and Wildlife (Ministère des forêts et de la faune). Local chiefs and local people gave permission to collect samples in non-protected areas. No specific permission was required for locations outside the protected areas and field studies did not involve endangered or protected species.

Study area

The coast of Cameroon is about 400 km long, stretching from the country's border with Equatorial Guinea in the south to its northern border with Nigeria, on the Eastern Atlantic coast. This coastline has an interesting geomorphological history and a coastal hydrology that is characterized by a dense network of rivers. The Cameroon Volcanic Line (CVL) is a 1600 to 1800 km chain of volcanoes [54, 55] that started forming about 30 Ma BP and stretches from far inland in the north, via Mount Cameroon and Mount Etinde across the Cameroonian Atlantic coast, to the Bioko, Príncipe, São Tomé, and Annobón Islands [56]. The CVL separates the mangroves of the present-day Rio Del Rey Estuary in the north from those of the Cameroon Estuary complex (CEC) and other southerly-situated populations (Fig 1). Bioko Island is the youngest of all these islands, having formed about 1 Ma BP, and it is situated *ca.* 40 km from the edge of the continental shelf at less than 60 m below sea level [56, 57]. It was repeatedly connected to mainland Cameroon during glacial times [56–58]. Following glacial retreat *ca.* 12 ka BP, sea level rose and covered these lowlands, separating Bioko from the mainland [56–58] and forming the Inter-Bioko-Cameroon (IBC) corridor. In addition to the many rivers flowing into the coastal waters of Cameroon, the isolation of Bioko Island from the mainland has caused ocean swells around the coast of Cameroon to be weak [59]. The tidal system in our study site is semidiurnal, ranging in amplitude between 0.3 m and 3 m, depending on the locality [59, 60]. Ocean currents near the coast of Cameroon are characterized by the convergence of the south-eastwards flowing Guinea Current and the northwards surface flow, converging near the CEC (Fig 1). Four disjunct mangrove areas (estuaries) currently exist along the coast of Cameroon with *Rhizophora racemosa* (90%) and *Avicennia germinans* L. (5%) being the predominant mangrove species on this coastline [61]. Hence, this study on genetic patterns of a widespread mangrove species, *R. racemosa*, reveals the importance of geomorphological history and ocean currents in shaping contemporary genetic structure.

Sampling and genotyping

Leaf tissue was collected from adult trees at least 10 m apart along transects (parallel to the direction of river flow), except at Mabeta where only fringing stands were left, hampering continuous transects. Hence, in the latter area, all adult individuals were sampled. On average, 30 adult trees were sampled per transect and transects in each site were pooled into a single population, except for areas where only one transect could be obtained due to very few stands (Ekondo-Titi and Mabeta). Three populations were sampled from the Rio Del Rey Estuary in the north (Ekondo-Titi, Mbongo, Bekumu), six populations from the CEC at the center (Mabeta, Tiko, Douala Akwa-Nord, Douala Bonamoussadi, Douala Bonaberi, Douala-Edea Reserve). The Kibi population from the Lokoundje Estuary (with transects from Londji and Mpalla), and the Campo population from the Ntem Estuary (with transects from Ipono and Campo Beach) (see Table 1, Fig 1, Fig 2). Leaf samples were kept dry on silica gel. Genomic DNA was extracted from dried leaf tissue using the E.Z.N.A SP plant DNA Mini Kit (Omega

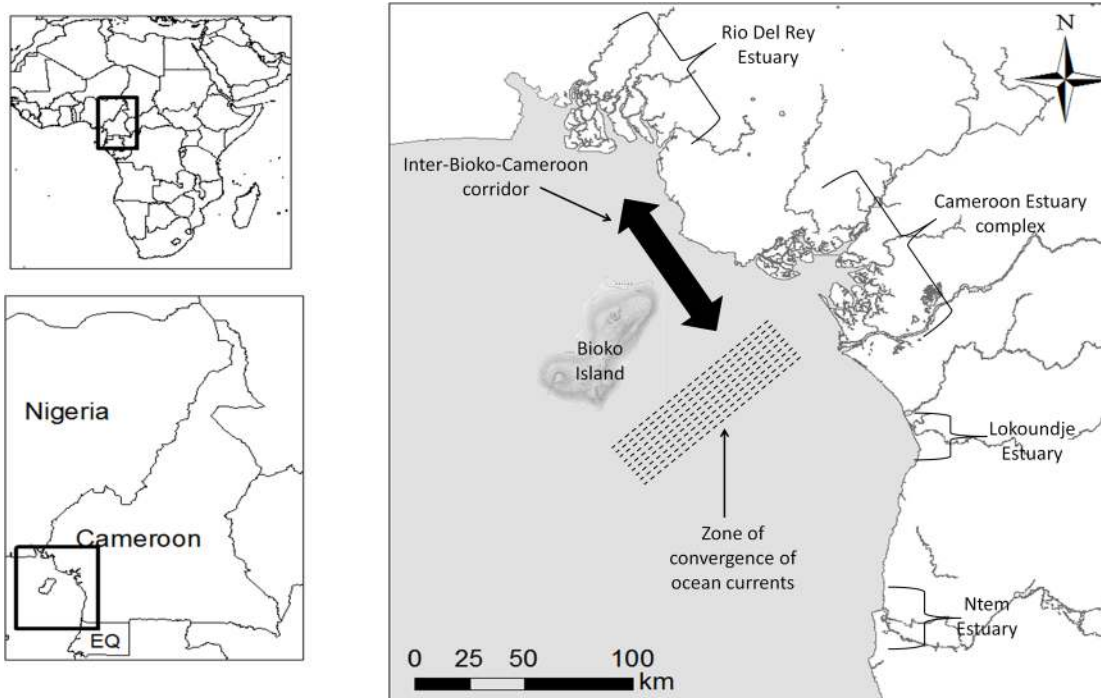


Fig 1. The coastal area of Cameroon indicating the studied estuaries and major dispersal corridor and barrier to gene flow. Map generated from Hydrography shape files obtained from the World Resource Institute (WRI) Congo Basin Forest Atlases webpage: <http://www.wri.org/our-work/project/congo-basin-forests/cameroon>.

doi:10.1371/journal.pone.0150950.g001

bio-tek). Eleven (11) polymorphic microsatellite markers (Rrace1, Rrace3, Rrace5, Rrace6, Rrace7, Rrace12, Rrace15, Rrace17, Rrace18, Rrace20, and Rrace24) initially developed from Cameroonian populations of *R. racemosa* [62], were used in a single multiplex for the Polymerase Chain Reaction (PCR). The PCR reactants were 1.25 µl of the primer mix, 6.25 µl of the Master mix, 2.5 µl of H₂O, and 3 µl of DNA, in a final volume of 13 µl. The PCR reaction conditions were: an initial denaturation of 95°C for 15 minutes followed by an extension of 30 seconds at the same temperature. Annealing was then allowed at a temperature of 57°C, followed

Table 1. Description of the studied *R. racemosa* populations from the coastline of Cameroon.

Estuary	Site No.	Sites (Region)	Pop ID	Latitude	Longitude	Notes	Habitat type
Rio Del Rey Estuary	1	Ekondo-Titi	EKO	4°46'18.88" N	8°47'52.84" E	S, D,	Riverine
	2	Mbongo, Bekiri Beach	MBO	4°29'34.41" N	8°55'51.00" E	L,U	Riverine
	3	Bekumu	BEK	4°22'49.84" N	8°53'46.45" E	L, D	Estuarine
Cameroon Estuary (CEC)	4	Mabeta Njanga	MAB	3°57'53.09" N	9°15'58.06" E	S, D,	Coastal
	5	Tiko beach	TIKO	4°03'30.02" N	9°22'56.06" E	L, D	Riverine
	6	Douala, Akwa-Nord	AKN	4°05'23.76" N	9°43'19.24" E	S, D,	Riverine
	7	Douala, Bonamoussadi	SADI	4°06'51.60" N	9°44'58.07" E	S, D,	Riverine
	8	Douala, Bonaberi	BERI	4°04'40.70" N	9°42'16.31" E	S, D,	Estuarine
	9	Douala-Edea Reserve	RSVM	3°45'20.75" N	9°42' 0.26" E	L, U	Riverine
Lokoundje	10	Kribi, Londji & Mpalla	KRIBI	3°04'57.67" N	9°58'29.50" E	S, D,	Estuarine
Ntem	11	Campo Beach, Ipono	CAMPO	2°20'09.49" N	9°51'19.89" E	S, U,	Estuarine

S = small, L = Large, U = undisturbed, D = disturbed

doi:10.1371/journal.pone.0150950.t001

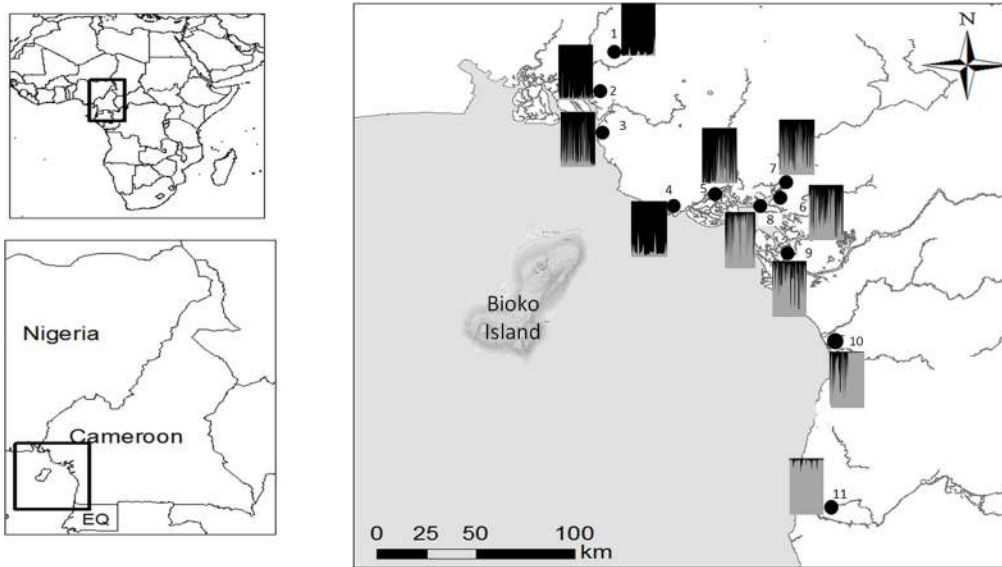


Fig 2. The coastal area of Cameroon with the 11 sites as in Table 1 and the proportions of two inferred clusters of individuals for each population. Proportions of inferred clusters (Q-values) per population are represented as bar charts at their respective geographical locations on the map.

doi:10.1371/journal.pone.0150950.g002

by an extension at 72°C. Subsequently, the initial steps were repeated with final extension time of 60°C for 30 minutes and a cooling to 4°C for 1 minute in a Bio-Rad thermal cycler (MJ research PTC-200 and Bio-Rad MyCycler). Fragment analysis of PCR products was done by MacroGen Corporation (Seoul, South Korea). GeneMarker (SoftGenetics LLC, State College, USA) was used to score fragments.

Data quality and genetic diversity

Genotypic linkage disequilibrium between all pairs of loci was tested using FSTAT v.1.2 [63]. The presence of null alleles and significant deviations from Hardy-Weinberg equilibrium (HWE) were investigated for each locus and population with Genepop v.4.3 [64]. MICRO-CHECKER [65] was used to investigate scoring errors and allele dropouts. We calculated allelic richness (A_r) and significance of heterozygote deficiency (F_{is}) based on Bonferroni corrections with FSTAT. Rarefaction of allelic richness was to the smallest population size (smallest sample = 30). The observed and expected heterozygosity were calculated using GenAlex v.6.5 [66]. The total number of alleles and number of effective alleles per population was obtained from GenAlex. We tested populations for recent bottleneck events with the software BOTTLENECK v.1.2.02 [67]. This was done with 1000 iterations by testing the assumptions that: mutation rate of microsatellite markers follow (1) an Infinite Allele Model (IAM); (2) a Stepwise Mutation Model (SMM); or (3) a Two Phase Model (TPM) (TPM assumes 70% SMM rate and a variance of 30%).

Genetic structure

Global mean population differentiation (Θ) and inbreeding (f) over all loci [68] was estimated using FSTAT. Genetic differentiation, at first, was tested by a hierarchical analysis of molecular variance (AMOVA-Fst) calculated with GenAlex, where populations were grouped according to their estuary, and also by an AMOVA without any prior grouping into estuaries. Secondly, a Bayesian clustering analysis at individual level was conducted in STRUCTURE v.2.3.4 [69]

following the admixture model by testing K values ranging from 1 to 10 without any prior indication of population origin, with 10 iterations per K value. The length of burn-in period was set at 10 000 and the number of Markov Chain Monte Carlo (MCMC) repeats after burning at 1 000 000. The program minimizes deviations from the Hardy Weinberg Equilibrium (HWE) and linkage equilibrium. The results of K values were obtained from STRUCTURE HARVEST [70] and the Evanno method of the highest ΔK value [71] was used to determine the best K value. We also calculated pairwise genetic differentiation (Fst) with GenAlex and pairwise allelic differentiation (D_{est}) using SMOGD online <http://www.ngcrawford.com/django/jost/> [72], for all population pairs. Also patterns of the spatial relationship among populations was done by Principal Coordinate Analysis (PCoA) with GenAlex and by a Neighbor-joining (NJ) tree based on Nei's genetic distances [73] as computed with POPTREE v.2 [74], bootstrapping at 10000.

Hypotheses testing

The Cameroon Volcanic Line is a barrier to gene flow vs the Inter-Bioko-Cameroon corridor as a pathway for gene flow. It is expected that (1) if the CVL presents a barrier to gene flow, populations on either side of this barrier will be genetically isolated from each other and (2) if the Inter-Bioko-Cameroon corridor is a pathway for gene flow, populations will be admixed. To test this, we first created a predictor matrix whereby population pairs consisting of one population to the north and another to the south of this barrier were coded as 1 (high expected differentiation), while those with pairs located on the same side, either north or south, were coded as 0 (low expected differentiation), similar to the methodology applied by Dodd *et al.* [36] and Wee *et al.* [53]. This predictor matrix and a matrix of pairwise Fst were then used together in a Mantel test with 9999 permutations in GenAlex. Using BayesAss ed. 3 [75], we estimated contemporary migration (dispersal) rates and directionality between populations on either side of the supposed barrier or present-day corridor to check for connectivity between these areas. The program was run at 3×10^6 MCMC iterations with a burn-in period of 10^6 at a sampling frequency of 2000. This software allows only for the estimation of recent migration rates, *i.e.* within the past 3 generations [38].

The convergence zone of two currents at the Cameroon Estuary complex is a barrier to gene flow. We expect that if the zone of convergence of the Guinea Current and the northward flowing surface current is a barrier to gene flow, there will be a genetic discontinuity and an absence of migration between populations on either side of the barrier. Contemporary migration (dispersal) rates were calculated following the same parameters and software programs as above. We tested for Isolation by distance-related dispersal limitation (IBD) at population level through a Mantel test of pairwise actual genetic (allelic) differentiation using D_{est} [76] (SMOGD online) versus pairwise direct flight geographical distances (km) with 9999 permutations in GenAlex. Considering the LDD potential of *Rhizophora* species and the regional scale of our study (*i.e.*, 11 study sites located along 400 km of coastline), we decided to check whether or not dispersal is limited by physical barriers rather than by geographic distance. We therefore calculated barriers to gene flow using the software program Barrier v.2.2 [77] based on information from 3 matrices (Fst, D_{est} , and Nei's genetic distances between populations) following an *a priori* assignment of 3 barriers: (1) the CVL; (2) the ocean current convergence zone; and (3) geographical distance. This program runs the Monmonier maximum difference algorithm on a genetic distance matrix (or matrices) and geographical coordinates of sampling locations to detect genetic breaks (*i.e.*, genetic barriers) based on *a priori* number of barriers set by the user. Due to the likely inbreeding signals observed in the Kribi population, this population was omitted and a second run was conducted using Barrier to assess whether or not the

barriers observed in the first run were due to inbreeding signals. Also, to identify the major barrier to gene flow we did a third run with only one *a priori* barrier set. Following Dodd *et al.* [36] and Wee *et al.* [53], and similar to the first hypothesis above, a new predictor matrix of population pairs on either side and on the same side of this convergence zone, was created, which was used in a Mantel test with a pairwise F_{st} matrix. We also carried out a partial Mantel test of three matrices: genetic distance matrix (F_{st}), geographic distance matrix, and the predictor matrix in IBDWS v. 3.23 online [78]. This allowed for investigating the significance of this convergence zone of ocean currents as a barrier to gene flow. To ascertain this, genetic differentiation (F_{st}) for all population pairs from within the same ocean current were classified as “Within” and pairs from different ocean currents (*i.e.*, from opposite sides of this barrier) as “Between”. Using this classification, the two groups were tested for significant difference in F_{st} using the Mann–Whitney U test in Statistica v.8 (StatSoft Inc., USA).

Additionally, gene flow patterns and genetic clusters from the STRUCTURE analysis were interpreted in the context of ocean surface currents from a mesoscale and tide-resolving configuration of the Massachusetts Institute of Technology general circulation model (MITgcm; [79]). The model has horizontal grid spacing of *ca.* 4 km and vertical grid spacing of 1 m near the surface in order to better resolve surface boundary layer currents. The simulation is initialized from a data-constrained global ocean solution provided by the Estimating the Circulation and Climate of the Ocean, Phase II (ECCO2) project [80]. At the surface the simulation is forced by six-hourly fields from the 0.14° (*i.e.*, 15 km or less) European Center for Medium-Range Weather Forecasts (ECMWF) atmospheric operational model analysis, starting in 2011. Tidal forcing for the 16 largest tidal constituents is also applied. The bathymetry is a blend of the Smith and Sandwell [81] version 14.1 and the International Bathymetric Chart of the Arctic Ocean (IBCAO).

Virtual propagules were released hourly for the months February, March, April, September and October 2012, being the general propagule release periods for *R. racemosa* in the study area (personal observation; observations in line with Menezes *et al.* [82] for Brazil). In total, 3626 virtual propagules were released in each of the 11 coastal locations. All virtual propagules were given a floating period of 3 months and were advected by surface currents from the numerical ocean simulation described above. These virtual 3-month propagule trajectories are used to interpret gene flow patterns and genetic clusters in this study.

The role of ocean current convergence on genetic diversity level. It is expected that at the convergence zone of both the Guinea and northward flowing ocean currents, genetic diversity will be higher because of the input of alleles (via propagules) from northerly and southerly mangrove populations. To test this, we pooled populations into estuary groups and tested for significant differences between groups in allelic richness, genotypic diversity and heterozygosity deficiency (F_{is}) in FSTAT. Since the Lokoundje and the Ntem Estuaries had just one population each, they were pooled into one group since they lie on the same trajectory of the northward flowing surface current (on the same side of the convergence zone).

Results

Data quality and genetic diversity

We found no linkage disequilibrium between any pair of loci. Null alleles could potentially be present in 3 loci at Kribi (site 10, frequency < 0.4) (S2 Table). Significant deviations from HWE were observed in 2 (Rrace5 and Rrace7) out of 11 Loci ($p < 0.001$), following the multi-population tests. Genetic diversity of *R. racemosa* populations from the Cameroonian coastline was low to moderate. The observed heterozygosity of the populations ranged from 0.169 to 0.369 (mean = 0.295) while the expected heterozygosity (H_e) ranged from 0.244 to 0.335

Table 2. Descriptive statistics of genetic diversity based on 11 nuclear microsatellite loci for 11 populations of *Rhizophora racemosa* from the Coast of Cameroon.

Site No.	Pop ID	Ntransect	N	At	Ae	Ar	Ho	He	Fis
1	EKO	1	30	28	1.6	2.5	0.339	0.312	-0.07
2	MBO	3	91	32	1.6	2.5	0.364	0.309	-0.17
3	BEK ^b	4	125	43	1.5	2.9	0.281	0.276	-0.012
4	MAB	1	31	27	1.4	2.4	0.284	0.25	-0.121
5	TIKO ^b	5	126	38	1.6	2.9	0.312	0.321	0.031
6	AKN ^b	3	125	36	1.6	2.7	0.281	0.285	0.02
7	SADI	5	141	36	1.6	2.7	0.302	0.309	0.024
8	BERI ^b	4	122	40	1.7	3	0.369	0.335	-0.095
9	RSVM	3	80	29	1.5	2.4	0.266	0.257	-0.028
10	KRIBI	2	57	25	1.5	2.1	0.169	0.244	0.316*
11	CAMPO ^b	2	52	34	1.5	2.8	0.281	0.285	0.027
	Mean	3	89	33.5	1.6	2.6	0.295	0.289	-0.039
	SE	0.4	4	1.7	0	0.1	0.022	0.019	0.038

^b indicates populations undergoing recent bottleneck (standardized difference test; $p < 0.001$), while

* indicates populations with significant Fis ($p < 0.05$). N = sample size, Ntransect = number of transects per population, At = total number of alleles, Ae = number of effective alleles, Ar = allelic richness, Ho = observed heterozygosity, He = expected heterozygosity, Fis = inbreeding coefficient.

doi:10.1371/journal.pone.0150950.t002

(mean = 0.290) (Table 2). The average allelic richness was 2.6 and was highest at BERI (site 8, Ar = 3.0), BEK (site 3, Ar = 2.9) and TIKO (site 5, Ar = 2.9). Kribi (site 10) had the lowest allelic richness (Ar = 2.1) and heterozygosity (Ho = 0.169) and was the only population with significant inbreeding coefficient (Fis = 0.316, $p < 0.05$). Five out of 11 populations gave signatures of recent bottlenecks ($p < 0.001$ under the standardized difference test for SMM) (Table 2).

Genetic structure

Jackknifing across loci showed that there was low overall genetic differentiation ($\Theta = 0.073$, SE = 0.019) and no inbreeding ($f = -0.007$, SE = 0.054). However, there was 6% variation among regions and 4% among populations following a hierarchical AMOVA-Fst (Table 3). Frt

Table 3. Analysis of Molecular Variance (AMOVA-Fst) based on a pooling of populations (Hierarchical) into estuaries and non-pooling (non-hierarchical).

Hierarchical based on grouping into estuaries						Non-hierarchical					
Source	df	SS	MS	Est. Var.	%	Source	df	SS	MS	Est. Var.	%
Among Estuaries	3	149.164	49.721	0.109	6%	Among Pops	10	254.577	25.458	0.136	8%
Among Pops	7	105.412	15.059	0.072	4%	Among Indiv	971	1620.773	1.669	0.008	0%
Among Indiv	971	1620.773	1.669	0.008	0%	Within Indiv	982	1622.5	1.652	1.652	92%
Within Indiv	982	1622.5	1.652	1.652	90%	Total	1963	3497.849		1.797	100%
Total	1963	3497.849		1.842	100%	F-Statistics	Value	P(rand > = data)			
F-Statistics	Value	P(rand > = data)				Fst	0.076	0.000			
Frt	0.059	0.001				Fis	0.005	0.293			
Fsr	0.041	0.001				Fit	0.08	0.000			
Fst	0.098	0.001				Nm	3.0				
Fis	0.005	0.304				F'st	0.108				
Fit	0.103	0.001									
Nm	2.3										

doi:10.1371/journal.pone.0150950.t003

Table 4. Pairwise population genetic differentiation.

	EKO	MBO	BEK	MAB	TIK	AKN	SADI	BERI	RSVM	KRIBI	CAMPO
EKO	0	0	0.001	0.006	0.003	0.01	0.004	0.014	0.015	0.055	0.062
MBO	0.000 ^{ns}	0	0.002	0.009	0.003	0.01	0.006	0.017	0.018	0.052	0.063
BEK	0.040	0.044	0	0.013	0.003	0.004	0.003	0.009	0.009	0.035	0.044
MAB	0.054	0.056	0.087	0	0.013	0.018	0.017	0.032	0.015	0.038	0.051
TIK	0.028	0.029	0.019	0.060	0	0.004	0.003	0.005	0.008	0.03	0.046
AKN	0.087	0.085	0.036	0.114	0.021	0	0.001	0.001	0.005	0.015	0.029
SADI	0.064	0.068	0.014	0.101	0.017	0.015	0	0.003	0.004	0.027	0.039
BERI	0.094	0.099	0.062	0.134	0.040	0.028	0.042	0	0.007	0.028	0.039
RSVM	0.110	0.118	0.078	0.122	0.048	0.044	0.057	0.044	0	0.021	0.024
KRIBI	0.202	0.190	0.164	0.204	0.121	0.086	0.115	0.112	0.121	0	0.009
CAMPO	0.239	0.234	0.217	0.265	0.177	0.133	0.155	0.153	0.176	0.062	0

(F_{st}) (below the diagonal) and allelic differentiation (D_{est}) (above the diagonal) between all possible pairs of populations. All significant at p < 0.001 and ^{ns} means non-significant differentiation between MBO and EKO

doi:10.1371/journal.pone.0150950.t004

(0.059) and F_{st} (0.098) were both low but significant at p < 0.001. The non-hierarchical AMOVA-F_{st} showed 8% variation among populations (F_{st} = 0.076) (Table 3). Bayesian clustering analysis assembled individuals into 2 clusters (K = 2, S1 Fig), with a very high degree of admixture of populations from the Rio Del Rey Estuary and those of the Cameroon Estuary complex (CEC) while those of the Lokoundje and the Ntem estuaries formed a different cluster (Fig 2). Pairwise F_{st} and D_{est} generally increased significantly (p < 0.001) with geographical distance of population pairs (Table 4). PCoA and NJ tree showed a complex spatial relationship among populations. Generally patterns were similar to those observed for Bayesian clustering analysis, as there was clustering (i.e., mixtures) of populations of the Rio Del Rey Estuary and those of the CEC while the Kribi and Campo (sites 10 and 11) populations of the Lokoundje and the Ntem estuaries respectively were grouped separately (Fig 3).

Hypotheses 1 and 2: Corridors for and barriers to gene flow

A Mantel test of the predictor matrix assuming the Cameroon Volcanic line (CVL) is a barrier to gene flow and pairwise F_{st} was non-significant (data not shown). Contemporary migration rates (Fig 4, S1 Table) were high between populations of the Rio Del Rey and CEC, while those of the Lokoundje and the Ntem estuaries are isolated from the others (no migration). These results are in line with the genetic structure pattern, where high levels of admixture among populations of the Rio Del Rey and CEC were observed. The IBD test was significant (Fig 5, S3 Fig), indicating dispersal limitation with geographical distance. Assuming the convergence of ocean currents around the CEC to be a barrier to gene flow, the predictor matrix following this barrier and pairwise F_{st} in a Mantel test was significant (R² = 0.631, p < 0.05). Partial mantel test was significant for genetic and geographic distances while controlling for the predictor matrix (r = 0.53, p < 0.05), as well as for genetic distance and predictor matrices, while controlling for geographical distance (r = 0.43, p < 0.05). This significance was confirmed by a significant Mann–Whitney U test (p < 0.001) when F_{st} of population pairs were grouped into pairs from within the same ocean currents (“Within”) and pairs from across the convergence zone barrier (“Between”) (Fig 6). Probabilistic estimates of propagule dispersal trajectories from our model suggest that propagules can go through the Inter-Bioko-Cameroon (IBC) corridor; they also suggest that, Bekumu (site 3) and, secondarily, Mbongo (site 2) are potentially major

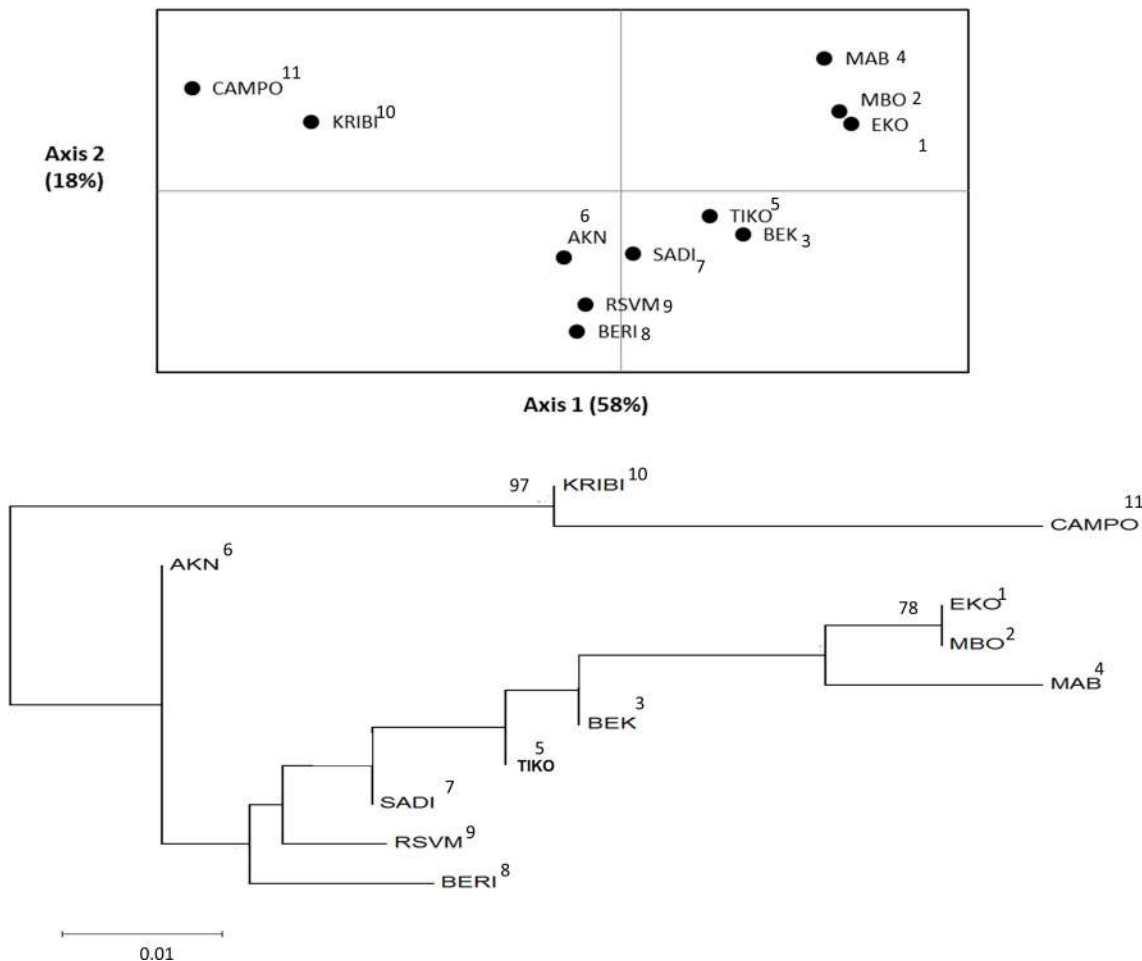


Fig 3. Principal Coordinate analysis (PCoA, above) and Neighbor-joining tree (NJ tree, below). The grouping of 11 populations of *Rhizophora racemosa* along the entire coast of Cameroon into 3 groups with high admixtures of populations from the Rio Del Rey Estuary and the Cameroon Estuary complex and isolation of first group of populations of the Loukondje Estuary (Kribi, site 10) and the Ntem Estuary (Campo, site 11). The second group is made-up of 2 landward populations from the Rio Del Rey Estuary (MBO, site 2 and EKO, site 1) (>75% bootstrapping). A third large group consisting of one seaward population from the Rio Del Rey Estuary (BEK, site 3) and 5 other populations from the Cameroon Estuary complex (sites 5–9). Bootstrap values ≥ 75 are indicated on each node of the NJ tree and site numbers (1–11) are indicated beside the pop ID's.

doi:10.1371/journal.pone.0150950.g003

source populations of propagules from the Rio Del Rey to the CEC (Fig 7). Model results also show that the convergence zone of currents represents a barrier to gene flow, as propagules from either side do not cross this barrier (Fig 7). Propagules from the CEC cover the shortest dispersal distances (Fig 7). A more holistic test to identify barriers to gene flow showed that the convergence zone of ocean currents is a barrier to gene flow (Fig 8), even after omitting the only (potentially) inbred population (Kribi, site 10) and after only one *a priori* barrier was used in the analyses (data not shown). Additionally, this test did not identify the CVL as a barrier to gene flow (Fig 8). Mabeta (site 4) was also isolated from all other populations (Fig 8). Ocean current patterns also illustrate the established IBC corridor is a pathway for connectivity between the CEC and the Rio Del Rey Estuary, and indicates as well the zone of convergence of the two ocean currents (S2 Fig).

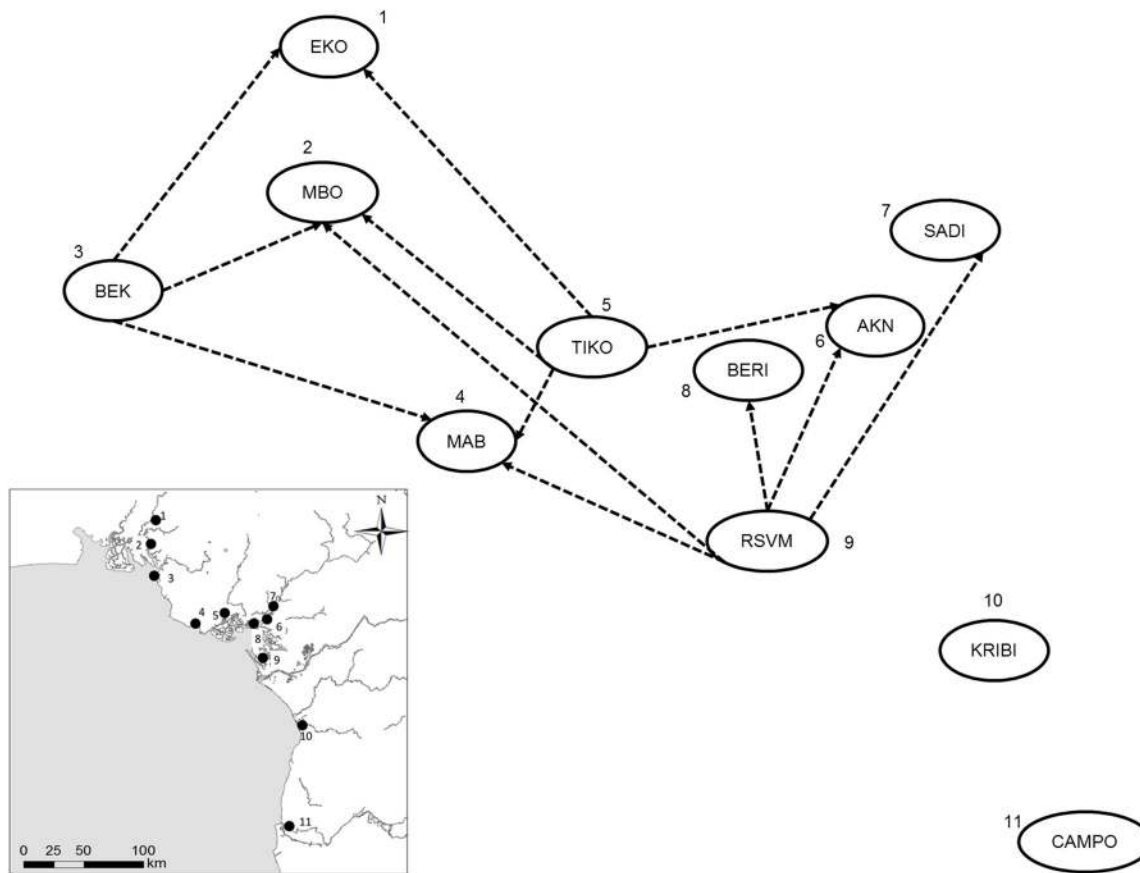


Fig 4. Pairwise contemporary migration rates between populations based on Bayesian estimates using individual multilocus genotypes.

doi:10.1371/journal.pone.0150950.g004

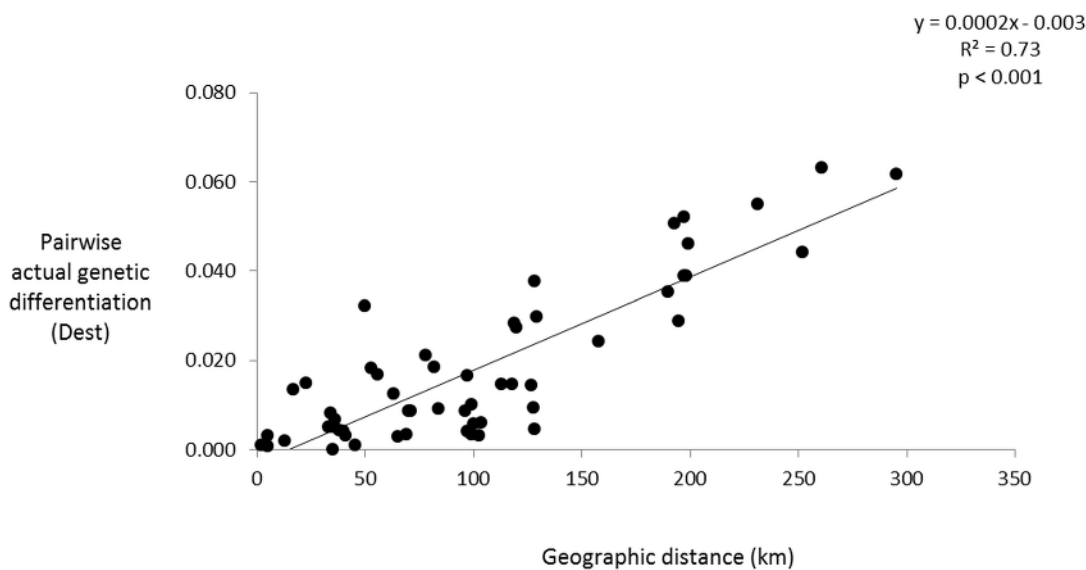


Fig 5. Strong isolation by distance (IBD) among *Rhizophora racemosa* populations along the coast of Cameroon. The pairwise actual genetic differentiation (D_{est}) increases from 0 to 7% over a direct flight geographic distance of up to 300 km, $p < 0.001$.

doi:10.1371/journal.pone.0150950.g005

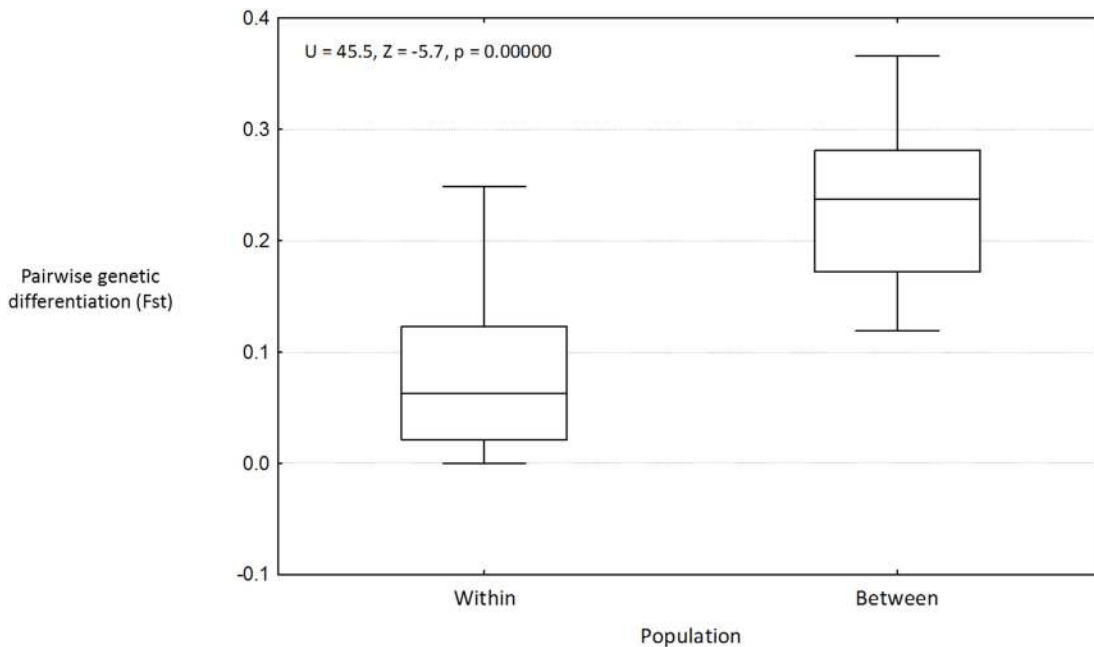


Fig 6. Box-whisker plot of mean population pairwise F_{st} values between “Within” ocean current population pairs group and ‘Between’ ocean current population pairs group.

doi:10.1371/journal.pone.0150950.g006

Hypothesis 3: Increased genetic diversity by convergence of two ocean currents at the Cameroon Estuary complex

Despite the large sample size of the Cameroon Estuary complex (CEC), there was no significant difference in genetic diversity parameters (A_r , H_o , H_s) among estuaries (Table 5). This indicates that there is no accumulation of genetic diversity in the CEC due to the convergence of ocean currents around this area (Table 5) or any other process. However, there was significant difference in inbreeding coefficient among estuary groups (F_{is} , at $p < 0.005$).

Discussion

The Inter-Bioko-Cameroon corridor facilitates gene flow between mangroves of the Rio Del Rey and the Cameroon Estuary complex

Our results are in line with the hypothesis that contemporary global mangrove distribution is shaped by (historical) vicariance and LDD [24, 39], and suggests that this applies as well to regional and local scales [62]. Bayesian clustering analysis shows high admixture of populations of the Rio Del Rey Estuary and those of the Cameroon Estuary complex (CEC). This is in accordance with the observed patterns of contemporary migration rates and modeled propagule dispersal trajectories and suggests that post-glacial SLR has established the genetic connectivity between populations of the Rio Del Rey Estuary and those of the CEC via the Inter-Bioko-Cameroon (IBC) corridor. *Rhizophora racemosa* is wind pollinated, with occasional insect pollination [83, 84]. Pollen dispersal by wind covers certain distances, but unlikely over the entire studied area. The efficiency of wind pollination is low in fragmented landscapes. This would imply restricted pollen dispersal for wind pollinated *Rhizophora* species, since mangroves are naturally patchy [85]. Additionally, mangrove habitats are generally heterogeneous landscapes, (e.g. interspersed by the landscape matrix of other forest or vegetation types) and this presents another strong barrier for most insect pollinators [85]. Furthermore, the

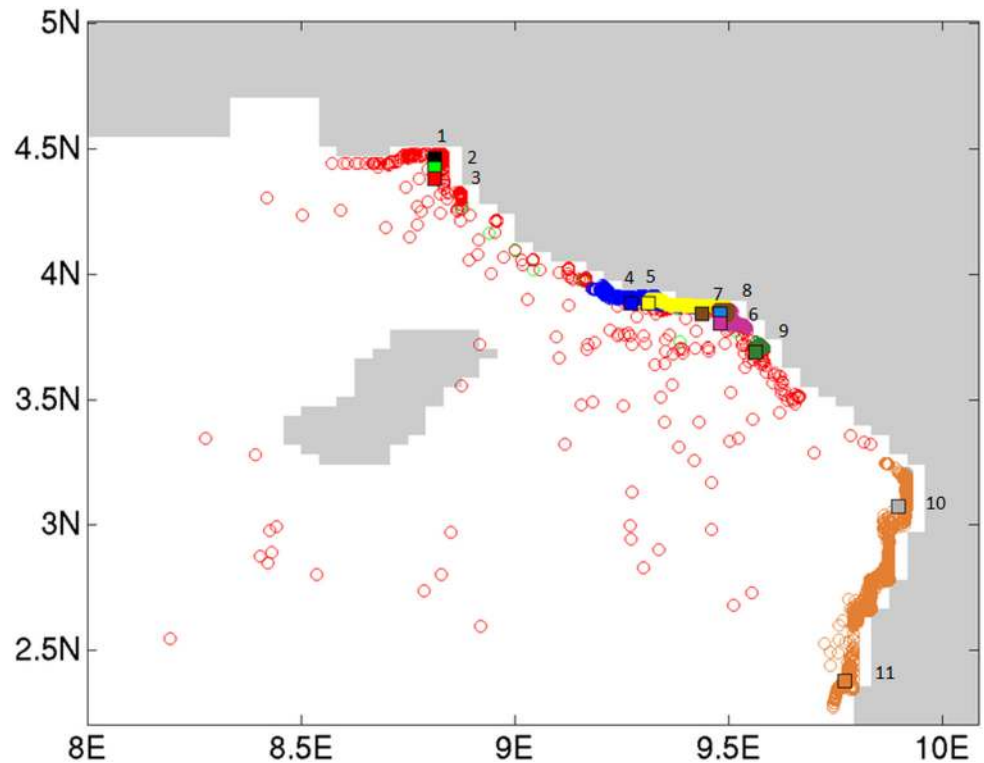


Fig 7. Location of virtual propagules (dots) after 3 months of floating. Virtual propagules were released hourly during the months February, March, April, September and October 2012, since these months correspond with propagule release periods for *Rhizophora racemosa* in the study area (personal observation). Hence, in total, 3626 virtual propagules were released in each of the locations. Author-defined release locations correspond with the localities where samples for our genetic analyses were collected, which were subsequently shifted to the closest ocean point (rectangles) to ensure the possibility of particle movement. Site numbers (1–11) are indicated beside the corresponding point.

doi:10.1371/journal.pone.0150950.g007

(historical) landscape was mountainous in nature (see Cameroon Volcanic Line). Although palaeo-weather conditions and wind directions are not known, this mountainous terrain (by acting as a wind shield) would have hardly allowed wind-borne pollen to cross over between the two formally separated estuaries. Nevertheless, potential gene flow between these two estuaries prior to the LGM cannot be completely excluded. Occasional fluctuations in sea levels prior to the LGM could have allowed for propagule exchange via the IBC corridor before its complete formation 12 ka BP. However, a period of 12 ka (*i.e.*, onset of the formation of the IBC corridor) provides a sufficiently long time period to generate the observed patterns of high connectivity between the Rio Del Rey and the CEC. This has resulted in reduced genetic differentiation between population pairs of the CEC and the Rio Del Rey, indicating that dispersal of propagules is more effective than pollen at preventing genetic divergence of populations (promoting homogeneity) [86]. Since seeds carry two alleles, their dispersal is twice as effective as the gene flow by pollen dispersal (if selection is ignored) [86]. Post-glacial mangrove shifts and expansion have mostly been attributed to the formation of favorable habitats by warmer temperatures at higher latitudes [8–10, 25, 27–29], accretion and favorable topographical conditions at landward margins [1, 7, 87]. Here, we present a case of connectivity between two mangrove estuaries through the formation of a corridor for gene flow, following post-glacial SLR. Our results from the Mantel tests, pairwise F_{st} , as well as the test of genetic barriers, indicate that the Cameroon Volcanic Line (CVL) does not represent a barrier to gene flow between

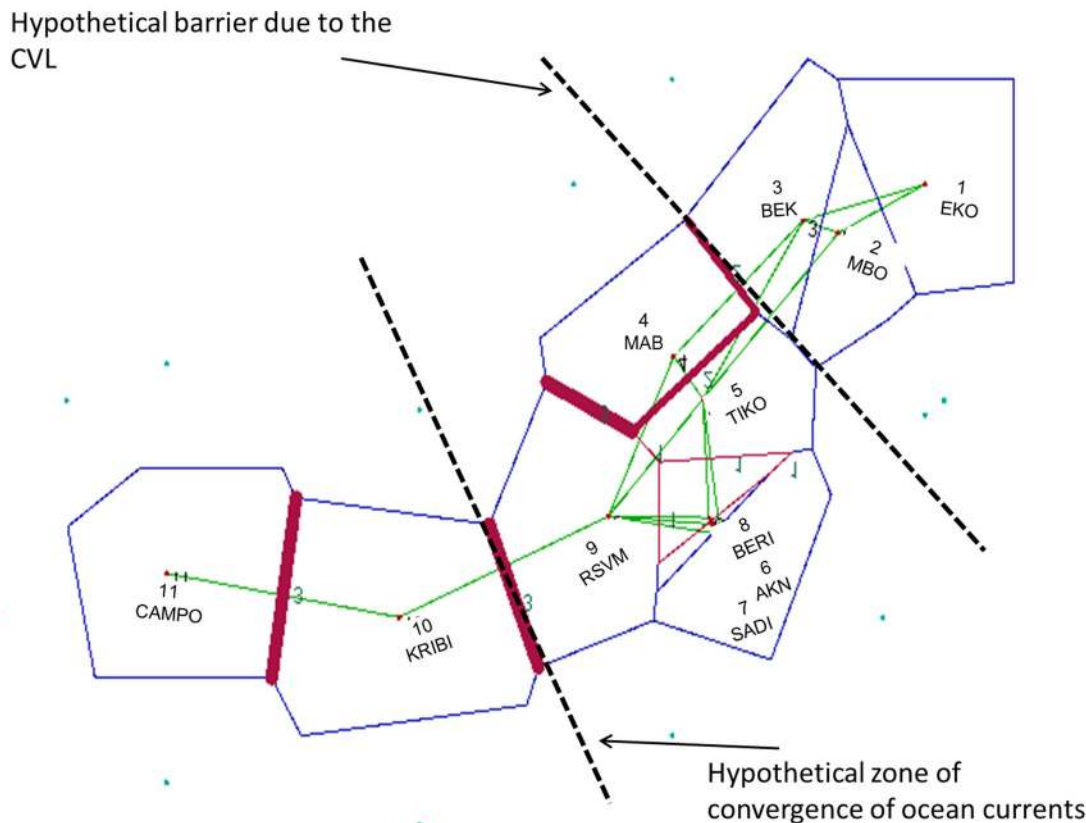


Fig 8. Gene flow barriers (red lines) and hypothetical barriers (Black dotted lines). The thickness of the red line indicates the importance of the barriers based on the 3 different distance matrices (pairwise Nei's genetic distances between populations (S3 Table), pairwise F_{st} , Pairwise D_{est}) used in the analysis.

doi:10.1371/journal.pone.0150950.g008

these two mangrove areas. Historically (> 13 ka BP), however, connecting Bioko Island to mainland Cameroon, the CVL presented an important land barrier that isolated the Rio Del Rey mangroves from those situated south of this barrier, since regional uplift and resulting land barriers are among the few impenetrable barriers to gene flow among seafaring organisms [50]. The present-day absence of this barrier underscores the functional role of the recently (< 12 ka BP) formed corridor following SLR, in facilitating gene flow between these two estuaries. The land bridge has not left any trace in genetic differentiation of mangrove populations of these two estuaries. Our results also show that (virtual) propagules of the CEC presently cover the shortest dispersal distances. This may be due to the tidal regimes in this area, preventing propagules from reaching the open ocean [62], hence reducing their potential to embark on

Table 5. Descriptive statistics of comparative genetic diversity of different estuaries.

Estuary	N	Ar	Ho	Hs	Fis*	Fst	Rel
Rio Del Rey	246	2.8	0.319	0.295	-0.082	0.035	0.074
CEC	627	2.7	0.307	0.304	-0.013	0.04	0.079
Ntem & Lokoundje	109	2.5	0.222	0.267	0.167	0.065	0.106

* Significance at $p < 0.01$ ($p = 0.004$).

doi:10.1371/journal.pone.0150950.t005

LDD. The role of tides in facilitating bidirectional gene flow along the Wouri River channel, for example, was highlighted by Ngeve *et al.* [62]. Understanding plant dispersal in riparian habitats provides important knowledge to understand how these areas are and had been colonized, and provides a hint on how they may respond to climate change [88]. Contemporary migration rates indicate that colonization of the Wouri River channel may have occurred following Slatkin's "propagule pool" model [42]) with the RSVM (site 9) (mangroves of the Douala-Edea Reserve) population being the most likely propagule source. Other populations of the CEC and the Rio Del Rey Estuary may have followed the "migrant pool" model [42]. Nevertheless, our results do not allow for conclusions on the colonization model for the southernmost and more diverged Kribi (site 10) and Campo (site 11) populations. Their source populations were not revealed, but it is likely that they have originated from mangroves in the Angola-Congo-Gabon range, borne by the northwards flowing surface currents.

Despite the resilience demonstrated by mangrove ecosystems to climate change, Ellison and Zouh [89] showed that recent climate change-induced SLR in Cameroon has resulted in die-backs in over two-third of seaward mangroves at a rate of about 3 m shoreline per year over the last 3 decades. According to Alongi [2] mangroves around the Cameroonian range (Central Africa) are among the least vulnerable to the effects of climate change globally, although reduction in subsidence, saline intrusion and SLR are assumed to be the most likely threats to negatively impact these mangroves [5]. However, we have indications that lowlands hampering gene flow during glacial times have been submerged by SLR, resulting in the connectivity of distantly located estuaries. Seasonal floods, expected to increase with changing climate, enhance the accessibility of mangrove forest by inhabitants of local communities, hence promoting mangrove exploitation [90]. Therefore, climate change, in addition to its impact on the area, on spatial distribution of suitable mangrove habitat and dispersal barriers, may influence the impacts from other anthropogenic drivers [2]. Future biogeographical range shifts will depend as well on the spatial variability of local extinction risk in response to environmental changes [5, 24], and other factors such as the geomorphological features of the locality [5].

The consequences of the IBC corridor for local mangroves are not obvious, since gene flow can either limit evolution by preventing local adaptation or facilitate evolution by spreading new genes and gene combinations throughout a range [91], except in areas where environmental constraints exert a selection pressure. However, the isolation of Bioko Island may be a remnant of range fragmentation of mangroves, at least if we assume that mangrove forests were ubiquitous in this region during glacial times. This is for example the case for the insect *Glossina palpalis palpalis*, where Bioko populations have been isolated, resulting in a unique clade, different from mainland populations [58]. Therefore, future studies should consider mangrove samples from Bioko to assess the full impact of the IBC corridor on genetic connectivity and potential range fragmentation of Central African mangrove populations. Nevertheless, there are indications that LDD via the IBC corridor, in addition to the time of its existence (*ca.* 12 ka), override patterns that might have existed prior to the LGM.

Ocean current patterns as a determinant of genetic structure

As hypothesized, ocean currents constitute an important determinant in understanding the observed regional genetic structure. This is expected, since ocean currents, in addition to pollen flow, represent the primary mechanism via which genetic material is exchanged among populations, close and remote. Ocean current patterns in our study area seem to underscore the genetic clusters that were detected using the Bayesian clustering, the pairwise F_{st} and D_{est} . Both the output from tests with genetic data and our probabilistic estimates from the numerical dispersal model, for example, support the movement of propagules from Bekumu (site 3) to

the more southerly (*ca.* 100 km) situated CEC. The southernmost populations, Kribi (site 10) and Campo (site 11), on the other hand seem to be lying “oceanographically” beyond the reach of the other populations in this region, explaining their genetic isolation.

Interestingly, while our genetic results reflect the absence of a contemporary barrier between the Rio Del Rey and CEC, numerical model output indicates that the genetic discontinuity between the CEC and the Kribi (site 10) and Campo (site 11) populations aligns with present-day ocean circulation in this area. Here, a linear convergence zone results from the confluence of ocean currents from the north and south. Ocean currents at the frontal zone are directed seaward, consequently preventing the exchange of propagules between localities north and south of it. The importance of considering ocean current patterns in explaining the genetic structure of coastal ecosystems has also been postulated by Wee *et al.* [53], who demonstrated that the genetic discontinuity between the mangrove populations of the Andaman Sea and the Malacca Strait is maintained by ocean features that prevent the mixing of water between these areas.

Considering ocean current velocities of 0.1 to 0.2 m s⁻¹ and geographical distances among the various estuaries in our study area (Rio Del Rey, CEC, Lokoundje and Ntem) on the order of 100 km, propagules could be transported between two neighboring populations in about 6 to 12 days. This is indeed an oversimplification, since dispersal vector properties (in this case ocean surface current speed and direction) vary over the course of a propagule’s dispersal trajectory. However, it demonstrates that within reported floating and viability periods for *Rhizophora* species, ranging from several weeks to several months [92–96], there is a sufficiently long period of time to reach remote areas; although our results demonstrate that this does not guarantee connectivity. Hence, the concept of isolation by oceanographic distance (*sensu* Wood [97]), more than just distance, may be a more appropriate and realistic model to explain the genetic structure of seafaring organisms. Since this model takes into account variations in dispersal vector properties, genetic breaks among proximate populations of species with propagules that can float for several months can be much better understood (see also [53]). The importance of oceanographic features, such as cyclonic and anticyclonic eddies in quantifying the dispersal trajectories of biological material at the ocean surface, has been mentioned in earlier oceanographic studies in the Mozambique Channel [98, 99]. This was reported as well by Wee *et al.* [53] in explaining the observed genetic structure in Southeast Asian mangroves. Here, we demonstrate that ocean convergence zones in coastal areas can act as a barrier for connectivity, and underscore the strength and complementarity of genetic and modeling studies. Hence, our study clearly indicates that knowledge of ocean circulation constitutes primary knowledge in the study of observed genetic structure of ocean-dispersed organisms. The combination of genetic data and model output, as well as empirical data from release-recapture methods, has been proposed earlier as a way to gain insight on (long distance) dispersal (see [12, 53, 100]). Others have demonstrated the value and strength of mathematical dispersal models to study oceanographic dispersal and connectivity in coastal areas at regional and global scales [97, 101–104] at which the use of release-recapture methods can hardly be applied (but see [105]).

Ocean convergence does not increase genetic diversity at the Cameroon Estuary complex

Moderate genetic diversity was observed in the red mangroves of the Cameroonian coastline and there was a general trend of genetic diversity parameters, decreasing from north to south. This may indicate that the relatively smaller populations in the Lokoundje (Kribi site 10) and Ntem (Campo, site 11) estuaries, located on the south of this coastline, have lower effective population sizes. Genetic diversity is directly proportional to effective population size [106,

[107]. Several populations were observed to be under recent bottleneck, likely as a result of high anthropogenic pressures on these coastal ecosystems [17, 18, 60, 108, 109]. Heterozygosity was moderate to low, and this has been commonly observed in *Rhizophora* species [62, 110, 111]. Generally, low heterozygosity can be attributed to several factors [cf. 36, 47, 48, 110]. Ng *et al.* [110] and Wee *et al.* [111] observed low heterozygosity to be in agreement with the biology of *Rhizophora* species. Null alleles are relatively common in microsatellite analysis [112] and they could be present at some loci in our study populations, albeit at very low frequencies (S2 Table). The number of effective alleles and mean number of alleles in all populations was low (means: $A_e = 1.6$, $A_d = 3$) so it is unlikely that null alleles will account for reduced heterozygosity. Null allele frequencies were highest in Kribi (site 10) for the Loci Rrace5 and Rrace6. Rrace5 deviates from HWE and this population has a significant inbreeding coefficient (Fis). So the potentially (relatively) high null allele frequencies at this population are most likely an over estimation because the significant Fis of this population and the deviation of this loci from HWE [113]. Significant Fis in the Kribi (site 10) population could be explained from either Wahlund-effect or potential inbreeding in the small, highly fragmented adult stands that made up the transect from Londji.

The highest genetic diversity was observed in the BERI (site 8), BEK (site 3), and TIK (site 5) populations and this could be due to propagule supply from upstream populations into these seaward populations (BERI and BEK) [62]. These two sites are part of the CEC. We expected that due to the presence of an oceanographic convergence just off the CEC, genetic diversity would be significantly higher at the CEC via the supply of propagules from both sides. There was no significant difference in the genetic diversity (A_r and H_o) of the CEC over other estuaries, despite the large sample size of the CEC. Thus, locally, river and coastal currents increase genetic diversity of the downstream populations of the Wouri River [62], but regionally, the CEC is not significantly different in genetic diversity from the other studied areas. *Rhizophora* propagules have quicker establishment chances and longer viability periods [114]. Despite the high fecundity of mangroves [115], low seed dispersal effectiveness (SDE) can result when the probability for dispersed propagules to remain viable along their dispersal trajectory is low and the potential for successful establishment after stranding is limited [116]. Hence, a plausible explanation is that many viable propagules are transported to the open sea and sink rather than projected suitable habitats where they could strand and eventually establish.

Conclusion

We found sufficient evidence to conclude that climate change-induced SLR in the recent past has created a corridor for gene flow between *Rhizophora racemosa* populations of the Rio Del Rey Estuary and those of the Cameroon Estuary complex. In contrast, our study illustrates how ocean features such as convergence zones in coastal areas can greatly influence the overall genetic structure in a particular region. The isolation by distance signals observed is likely isolation by resistance posed by the presence of an oceanic convergence zone, which was found to be an effective barrier to gene flow, hampering the exchange of propagules between populations at both sides of this barrier. Contrary to expectation, the convergence of two ocean currents did not result in higher genetic diversity at the Cameroon Estuary complex, likely as a result of ineffective overall dispersal.

Supporting Information

S1 Fig. Selecting the best K value using the Evanno method of delta K (a) and Ln(P) (b). (TIF)

S2 Fig. Ocean current simulated patterns of the coast of Cameroon. The convergence zone of the two currents offshore of the Cameroon Estuary complex is clearly revealed.

(TIF)

S3 Fig. Isolation by Distance based on pairwise Nei's genetic distances of populations and geographic distance.

(TIF)

S1 Table. Pairwise contemporary migration rates between population based on Bayesian estimates using individual multilocus genotypes. Significant migration rates are highlighted in bold. (DOC)

(DOCX)

S2 Table. Estimate of null allele frequency in all Loci for all studied populations. (DOC)

(DOCX)

S3 Table. Pairwise Nei's genetic distances of populations. (DOC)

(DOCX)

Acknowledgments

We extend sincere gratitude to Ma Christiana Nalova Ngenye, Mr. and Mrs. Ndoko Joseph (Ekondo-Titi), Pr. and Mrs. Oben Samuel (Bekumu), Mr. Peter Elive Ikome (Douala), Pr. Eban Daniel, Pr. Ntakim Clarence, Rev. Okala Dieudonne Bienvenue, Pr. and Mrs. Atiko Pierre (Kribi), Elder Atkin Egbe Obie (Kribi), Eugene N. Ngeve, and Ms Natalie Kana for logistical and field assistance. We are also grateful to Tim Sierens for technical and laboratory assistance. The numerical ocean modeling component of this research was carried out at the Jet Propulsion Laboratory, California Institute of Technology, under a contract with the National Aeronautics and Space Administration (NASA).

Author Contributions

Conceived and designed the experiments: MNN. Performed the experiments: MNN TVdS. Analyzed the data: MNN. Contributed reagents/materials/analysis tools: MNN TVdS DM LT. Wrote the paper: MNN TVdS. Originally formulated the idea: MNN NK LT. Collected the samples: MNN. Reviewed the manuscript: MNN TVdS DM NK LT.

References

1. Godoy MDP, Lacerda DD. Mangroves Response to Climate Change: A Review of Recent Findings on Mangrove Extension and Distribution. *An Acad Bras Cienc.* 2015; 87: 651–667. doi: [10.1590/0001-3765201520150055](https://doi.org/10.1590/0001-3765201520150055) PMID: [25993360](https://pubmed.ncbi.nlm.nih.gov/25993360/)
2. Alongi DM. Mangrove forests: resilience, protection from tsunamis, and responses to global climate change. *Estuarine, Coastal and Shelf Science.* 2008; 76: 1–13.
3. Alleman LK, Hester MW. Reproductive ecology of black mangrove (*Avicennia germinans*) along the Louisiana coast: propagule production cycles, dispersal limitations, and establishment elevations. *Estuaries and Coasts.* 2011; 34: 1068–1077.
4. Comeaux RS, Allison MA, Bianchi TS. Mangrove expansion in the Gulf of Mexico with climate change: Implications for wetland health and resistance to rising sea levels. *Estuarine, Coastal and Shelf Science.* 2012; 96: 81–95.
5. Alongi DM. The impact of climate change on mangrove forests. *Curr. Clim. Change Rep.* 2015; 1:30–39.
6. Friess DA, Krauss KW, Horstman EM, Balke T, Bouma TJ, Galli D, Webb EL. Are all intertidal wetlands naturally created equal? Bottlenecks, thresholds and knowledge gaps to mangrove and salt-marsh ecosystems. *Biological Reviews.* 2011; 87, 346–366. doi: [10.1111/j.1469-185X.2011.00198.x](https://doi.org/10.1111/j.1469-185X.2011.00198.x) PMID: [21923637](https://pubmed.ncbi.nlm.nih.gov/21923637/)

7. Peterson JM, Bell SS. Saltmarsh Boundary Modulates Dispersal of Mangrove Propagules: Implications for Mangrove Migration with Sea-Level Rise. PLoS ONE. 2015; 10: e0119128. doi: [10.1371/journal.pone.0119128](https://doi.org/10.1371/journal.pone.0119128) PMID: [25760867](https://pubmed.ncbi.nlm.nih.gov/25760867/)
8. Perry CL, Mendelsohn IA. Ecosystem effects of expanding populations of *Avicennia germinans* in a Louisiana salt marsh. Wetlands. 2009; 29: 396–406.
9. Quisthoudt K, Adams J, Rajkaran A, Dahdouh-Guebas F, Koedam N, Randin CF. Disentangling the effects of global climate and regional land-use change on the current and future distribution of mangroves in South Africa. Biodiversity and Conservation. 2013; 22: 1369–1390.
10. Cavanaugh KC, Kellner JR, Forde AJ, Gruner DS, Parker JD, Rodriguez W and Feller IC. Poleward expansion of mangroves is a threshold response to decreased frequency of extreme cold events. PNAS. 2014; 111: 723–727. doi: [10.1073/pnas.1315800111](https://doi.org/10.1073/pnas.1315800111) PMID: [24379379](https://pubmed.ncbi.nlm.nih.gov/24379379/)
11. IPCC. Climate Change 2007: Synthesis Report. Contribution of Working Groups I, II and III to the Fourth Assessment Report of the Intergovernmental Panel on Climate Change [Core Writing Team, Pachauri R.K, Reisinger A. (eds.)]. IPCC., 2007; Geneva, Switzerland, 104 pp.
12. Nathan R, Schurr FM, Spiegel O, Steinitz O, Trakhtenbrot A and Tsoar A. Mechanisms of long-distance seed dispersal. Trends in Ecology and Evolution. 2008; 23: 638–647. doi: [10.1016/j.tree.2008.08.003](https://doi.org/10.1016/j.tree.2008.08.003) PMID: [18823680](https://pubmed.ncbi.nlm.nih.gov/18823680/)
13. Dahdouh-Guebas F, Jayatissa LP, Di Nitto D, Bosire JO, Lo Seen D, Koedam N. How effective were mangroves as a defence against the recent tsunami? Curr Biol. 2005; 15: 443–447.
14. Nagelkerken I, van der Velde G, Gorissen MW, Meijer GJ, van't Hof T, den Hartog C. Importance of mangroves, seagrass beds and the shallow coral reef as a nursery for important coral reef fishes, using a visual census technique. Estuarine, Coastal and Shelf Science. 2000; 51: 31–44.
15. Nagelkerken I, Blaber SJM, Bouillon S, Green P, Haywood M, Kirton LG et al. The habitat function of mangroves for terrestrial and marine fauna: A review. Aquat. Bot. 2008; 89: 155–185.
16. Walters BB, Rönnbäck P, Kovacs JM, Crona B, Hussain SA, Badola R et al. Ethnobiology, socio-economics and management of mangrove forests: a review. Aquatic Bot. 2008; 89: 220–236.
17. Nfotabong-Atheull A, Din N, Longonje SN, Koedam N, Dahdouh-Guebas F. Commercial activities and subsistence utilization of mangrove forests around the Wouri estuary and the Douala-Edea reserve (Cameroon). Journal of Ethnobiology and Ethnomedicine. 2009; 5 doi: [10.1186/1746-4269-5-35](https://doi.org/10.1186/1746-4269-5-35)
18. Nfotabong-Atheull A, Din N, Koum LGE, Satyanarayana B, Koedam N, Dahdouh-Guebas F. Assessing forest products usage and local residents' perception of environmental changes in peri-urban and rural mangroves of Cameroon, Central Africa. Journal of Ethnobiology and Ethnomedicine. 2011; 7:41 doi: [10.1186/1746-4269-7-41](https://doi.org/10.1186/1746-4269-7-41) PMID: [22146073](https://pubmed.ncbi.nlm.nih.gov/22146073/)
19. Donato DC, Kauffman JB, Murdiyarto D, Kurnianto S, Stidham M, Kanninen M. Mangroves among the most carbon-rich forests in the tropics. Nature Geoscience. 2011; 4: 293–297. doi: [10.1038/ngeo1123](https://doi.org/10.1038/ngeo1123)
20. Spalding MD, Kainuma M, Collins L. World Atlas of Mangroves. Earthscan Ltd. 2010; London, UK.
21. Giri C, Ochieng E, Tieszen LL, Zhu Z, Singh A, Loveland T et al. Status and distribution of mangrove forests of the world using earth observation satellite data. Global Ecology and Biogeography. 2011; 20: 154–159.
22. Pernetta J. Mangrove forests, climate change and sea level rise: hydrological influences on community structure and survival, with examples from the Indo-West Pacific. Gland: IUCN, 1993, ISBN: 2-8317-0183-X.
23. Ellison AM, Farnsworth EJ, Merkt RE. Origins of mangrove ecosystems and the mangrove biodiversity anomaly. Glob. Ecol. Biogeogr. 1999; 8: 95–115.
24. Lo EY, Duke NC, Sun M. Phylogeographic pattern of *Rhizophora* (*Rhizophoraceae*) reveals the importance of both vicariance and long-distance oceanic dispersal to modern mangrove distribution. BMC Evol Biol. 2014; 14: 83. doi: [10.1186/1471-2148-14-83](https://doi.org/10.1186/1471-2148-14-83) PMID: [24742016](https://pubmed.ncbi.nlm.nih.gov/24742016/)
25. Pii MW, Boeger MRT, Muschner VC, Pie MR, Ostrensky A, Boeger WA. Postglacial north–south expansion of populations of *Rhizophora mangle* (*Rhizophoraceae*) along the Brazilian coast revealed by microsatellite analysis. American Journal of Botany. 2011; 98: 1031–1039. doi: [10.3732/ajb.1000392](https://doi.org/10.3732/ajb.1000392) PMID: [21653512](https://pubmed.ncbi.nlm.nih.gov/21653512/)
26. Quisthoudt K, Schmitz N, Randin CF, Dahdouh-Guebas F, Robert EMR, Koedam N. Temperature variation among mangrove latitudinal range limits worldwide. Trees. 2012; 26: 1919–1931.
27. Nettel A, Dodd RS. Drifting propagules and receding swamps: genetic footprints of mangrove recolonization and dispersal along tropical coasts. Evolution. 2007; 61: 958–971. PMID: [17439624](https://pubmed.ncbi.nlm.nih.gov/17439624/)
28. Triest L. Molecular ecology and biogeography of mangrove trees towards conceptual insights on gene flow and barriers: A review. Aquat. Bot. 2008; 89(2): 138–154.

29. Sandoval-Castro E, Dodd RS, Riosmena-Rodríguez R, Enríquez-Paredes LM, Tovilla-Hernández C, López-Vivas JM et al. Post-Glacial Expansion and Population Genetic Divergence of Mangrove Species *Avicennia germinans* (L.) Stearn and *Rhizophora mangle* L. along the Mexican Coast. *PLoS One*. 2014; 9(4): e93358. doi: [10.1371/journal.pone.0093358](https://doi.org/10.1371/journal.pone.0093358) PMID: [24699389](https://pubmed.ncbi.nlm.nih.gov/24699389/)
30. Castillo-Cárdenas MF, Toro-Perea N, Cárdenas-Henao H. Population genetic structure of neotropical mangrove species on the Colombian Pacific coast: *Pelliciera rhizophorae* (Pellicieraceae). *Biotropica*. 2005; 37: 266–273.
31. Saintilan N, Wilson NC, Rogers K, Rajkaran A, Krauss KW. Mangrove expansion and salt marsh decline at mangrove poleward limits. *Global Change Biology*. 2014; 20: 147–157, doi: [10.1111/gcb.12341](https://doi.org/10.1111/gcb.12341) PMID: [23907934](https://pubmed.ncbi.nlm.nih.gov/23907934/)
32. Gunn CR and Dennis JV. *World Guide to Tropical Drift Seeds and Fruits*. Krieger, 1999 ISBN 1-57524-147-1.
33. Randin CF, Paulsen J, Vitasse Y, Kollas C, Wohlgemuth T, Zimmermann NE, et al. Do the elevational limits of deciduous tree species match their thermal latitudinal limits?. *Global Ecology and Biogeography*. 2013; 22: 913–923
34. Dahdouh-Guebas F, Koedam N. Are the northernmost mangroves of West Africa viable?—A case study in Banc d'Arguin National Park, Mauritania. *Hydrobiologia*. 2001; 458(1–3): 241–253.
35. Balke T, Bouma TJ, Horstman EM, Webb EL, Erfteimeijer PLA, Herman PMJ. Windows of opportunity: thresholds to mangrove seedling establishment on tidal flats. *Mar. Ecol. Prog. Ser.* 2011; 440: 1–9.
36. Dodd RS, Afzal-Rafii Z, Kashani N, Budrick J. Land barriers and open oceans: effects on gene diversity and population structure in *Avicennia germinans* L. (Avicenniaceae). *Mol Ecol*. 2002; 11:1327–1338. PMID: [12144655](https://pubmed.ncbi.nlm.nih.gov/12144655/)
37. Cerón-Souza I, Bermingham E, McMillan WO, Jones FA. Comparative genetic structure of two mangrove species in Caribbean and Pacific estuaries of Panama. *BMC Evol. Biol.* 2012; 12:205. doi: [10.1186/1471-2148-12-205](https://doi.org/10.1186/1471-2148-12-205) PMID: [23078287](https://pubmed.ncbi.nlm.nih.gov/23078287/)
38. Cerón-Souza I, Gonzalez EG, Schwarzbach AE, Salas-Leiva DE, Rivera-Ocasio E, Toro-Perea N, Bermingham E et al. Contrasting demographic history and gene flow patterns of two mangrove species on either side of the Central American Isthmus. *Ecology and Evolution*. 2015; 5: 3486–3499. doi: [10.1002/ece3.1569](https://doi.org/10.1002/ece3.1569) PMID: [26380680](https://pubmed.ncbi.nlm.nih.gov/26380680/)
39. Duke NC, Lo EYY, Sun M. Global distribution and genetic discontinuities of mangroves—emerging patterns in the evolution of *Rhizophora*. *Trees*. 2002; 16: 65–79.
40. Orsini L, Vanoverbeke J, Swillen I, Mergeay J, Meester L. 2013. Drivers of population genetic differentiation in the wild: isolation by dispersal limitation, isolation by adaptation and isolation by colonization. *Molecular Ecol.* 22; 5983–5999.
41. Waters JM, Fraser CI, Hewitt GM. Founder takes all: density-dependent processes structure biodiversity. *Trends in Ecology and Evolution*. 2013; 28: 78–85. doi: [10.1016/j.tree.2012.08.024](https://doi.org/10.1016/j.tree.2012.08.024) PMID: [23000431](https://pubmed.ncbi.nlm.nih.gov/23000431/)
42. Slatkin M. Gene flow and genetic drift in a species subject to frequent local extinctions. *Theor Popul Biol.* 1977; 12: 253–262. PMID: [601717](https://pubmed.ncbi.nlm.nih.gov/601717/)
43. Meirmans PG. The trouble with isolation by distance. *Mol. Ecol.* 2012; 21: 2839–2846. doi: [10.1111/j.1365-294X.2012.05578.x](https://doi.org/10.1111/j.1365-294X.2012.05578.x) PMID: [22574758](https://pubmed.ncbi.nlm.nih.gov/22574758/)
44. Thomas L, Kennington WJ, Stat M, Wilkinson SP, Kool JT, Kendrick GA. Isolation by resistance across a complex coral reef seascape. *Proc. R. Soc. B*. 2015; 282: 20151217. <http://dx.doi.org/10.1098/rspb.2015.1217>. doi: [10.1098/rspb.2015.1217](https://doi.org/10.1098/rspb.2015.1217) PMID: [26224707](https://pubmed.ncbi.nlm.nih.gov/26224707/)
45. McRae BH. Isolation by resistance. *Evolution*. 2006; 60: 1551–1561. PMID: [17017056](https://pubmed.ncbi.nlm.nih.gov/17017056/)
46. Cerón-Souza I, Toro-Perea N, Cárdenas-Henao. Population genetic structure of Neotropical mangrove species on the Colombian Pacific Coast; *Avicennia germinans* (Avicenniaceae). *Biotropica*. 2005; 37:258–265.
47. Arnaud-Haond S, Teixeira S, Massa SI, Billot C, Saenger P, Coupland G et al. Genetic structure at range edge: low diversity and high inbreeding in Southeast Asian mangrove (*Avicennia marina*) populations. *Mol Ecol*. 2006; 15:3515–3525. PMID: [17032254](https://pubmed.ncbi.nlm.nih.gov/17032254/)
48. Arbeláez-Cortes E, Castillo-Cárdenas MF, Toro-Perea N, Cárdenas-Henao H. Genetic structure of the red mangrove (*Rhizophora mangle* L.) on the Colombian Pacific detected by microsatellite molecular markers. *Hydrobiologia*. 2007; 583: 321–330.
49. Mori GM, Zucchi MI, Souza AP. Multiple-Geographic-Scale Genetic Structure of Two Mangrove Tree Species: The Roles of Mating System, Hybridization, Limited Dispersal and Extrinsic Factors. *PLoS ONE*. 2015; 10(2): e0118710. doi: [10.1371/journal.pone.0118710](https://doi.org/10.1371/journal.pone.0118710) PMID: [25723532](https://pubmed.ncbi.nlm.nih.gov/25723532/)
50. Briggs JC, Bowen W. Marine shelf habitat: biogeography and evolution. *J. Biogeogr.* 2013; 40, 1023–1035. doi: [10.1111/jbi.12082](https://doi.org/10.1111/jbi.12082)

51. Su G, Huang Y, Tan F, Ni X, Tang T, Shi S. Genetic variation in *Lumnitzera racemosa*, a mangrove species from the Indo-West Pacific. *Aquat. Bot.* 2006; 84: 341–346.
52. Ayre DJ, Dufty S. Evidence for restricted gene flow in the viviparous coral *Seriatopora hystrix* on Australia's Great Barrier Reef. *Evolution.* 1994; 48: 1183–1201.
53. Wee AKS, Takayama K, Asakawa T, Thompson B, Sungkaew S, Tung NX, et al. Oceanic currents, not land masses, maintain the genetic structure of the mangrove *Rhizophora mucronata* Lam. (Rhizophoraceae) in Southeast Asia. *J Biogeogr.* 2014; 41: 954–964.
54. Elsheikh AA, Gao SS, Liu KH. Formation of the Cameroon Volcanic Line by lithospheric basal erosion: Insight from mantle seismic anisotropy. *Journal of African Earth Sciences.* 2013; 100: 96–108.
55. Adams AN, Wiens DA, Nyblade AA, Euler GG, Shore PJ, Tibi R. Lithospheric instability and the source of the Cameroon Volcanic Line: Evidence from Rayleigh wave phase velocity tomography. *Journal of Geophysical Research: Solid Earth.* 2015; doi: [10.1002/2014JB011580](https://doi.org/10.1002/2014JB011580)
56. Wronski T, Gilbert K, Long E, Michá B, Quinn R, Hausdorf B. Species richness and meta-community structure of land snails along an altitudinal gradient on Bioko Island, Equatorial Guinea. *Journal of Molluscan Studies.* 2014; 80: 161–168.
57. Wagner P, Leaché AD, Fujita MK. Description of four new West African forest geckos of the *Hemidactylus fasciatus* Gray, 1842 complex, revealed by coalescent species delimitation. *Bonn zoological Bulletin.* 2014; 63 (1): 1–14.
58. Cordon-Obras C, Cano J, Knapp J, Nebreda P, Ndong-Mabale N, Ncogo-Ada PR, et al. *Glossina palpalis palpalis* populations from Equatorial Guinea belong to distinct allopatric clades. *Parasites & Vectors.* 2014; 7: 31. doi: [10.1186/1756-3305-7-31](https://doi.org/10.1186/1756-3305-7-31)
59. Diop S, Barousseau J-P, Descamps C. The Land/Ocean Interactions in the Coastal Zone of West and Central Africa. *Estuaries of the World*, Springer. 2014 (June 4, 2014): ISBN-13: 978–3319063874.
60. Nfotabong-Atheull A, Din N, Dahdouh-Guebas F. Qualitative and quantitative characterization of mangrove vegetation structure and dynamics in a peri-urban settings of Douala (Cameroon): An approach using airborne imagery. *Estuaries Coast.* 2013; 36: 1181–1192.
61. Corcoran E, Ravillious C, and Skuja M. *Mangroves of Western and Central Africa*. UNEP-WCMC Biodiversity Series 26 2007. ISBN: 978-92-807-2792-0.
62. Ngeve MN, Sierens T, Koedam N, Triest L. Bidirectional gene flow on a river mangrove landscape and between-catchment dispersal of *Rhizophora racemosa* (Rhizophoraceae). 2016; submitted to *Aquatic Botany*
63. Goudet J. FSTAT (Version 1.2). A computer program to calculate F-statistics. *Journal of Heredity.* 1995; 86: 485–486.
64. Rousset F. GENEPOP'007: a complete re-implementation of the GENEPOP software for Windows and Linux. *Molecular Ecology Resources.* 2008; 8(1): 103–106. doi: [10.1111/j.1471-8286.2007.01931.x](https://doi.org/10.1111/j.1471-8286.2007.01931.x) PMID: [21585727](https://pubmed.ncbi.nlm.nih.gov/21585727/)
65. Van Oosterhout C, Hutchinson WF, Wills DPM, Shipley P. Micro-Checker: software for identifying and correcting genotyping errors in microsatellite data. *Mol. Ecol. Notes.* 2004; 4, 535–538.
66. Peakall R, Smouse PE. GenAlEx 6.5: genetic analysis in Excel. Population genetic software for teaching and research—an update. *Bioinformatics.* 2012; 28: 2537–2539. PMID: [22820204](https://pubmed.ncbi.nlm.nih.gov/22820204/)
67. Piry S, Luikart G, Cornuet JM. BOTTLENECK: a computer program for detecting recent reductions in the effective population size using allele frequency data. *J Hered.* 1999; 90:502–503. doi: [10.1093/jhered/90.4.502](https://doi.org/10.1093/jhered/90.4.502)
68. Weir BS, Cockerham CC. Estimating F-statistics for the analysis of population structure. *Evolution.* 1984; 38: 1358–1370.
69. Pritchard JK, Stephens M, Donnelly P. Inference of population structure using multilocus genotype data. *Genetics.* 2000; 155: 945–959. PMID: [10835412](https://pubmed.ncbi.nlm.nih.gov/10835412/)
70. Earl DA, vonHoldt BM. STRUCTURE HARVESTER: a website and program for visualizing STRUCTURE output and implementing the Evanno method. *Conservation Genetics Resources.* 2012; 4(2): 359–361 doi: [10.1007/s12686-011-9548-7](https://doi.org/10.1007/s12686-011-9548-7)
71. Evanno G, Regnaut S, Goudet J. Detecting the number of clusters of individuals using the software STRUCTURE: a simulation study. *Mol Ecol.* 2005; 14(8):2611–20. PMID: [15969739](https://pubmed.ncbi.nlm.nih.gov/15969739/)
72. Crawford NG. SMOGD: software for the measurement of genetic diversity. *Molecular Ecology Resources.* 2010; 10: 556–557. doi: [10.1111/j.1755-0998.2009.02801.x](https://doi.org/10.1111/j.1755-0998.2009.02801.x) PMID: [21565057](https://pubmed.ncbi.nlm.nih.gov/21565057/)
73. Nei M. Estimation of average heterozygosity and genetic distance from a small number of individuals. *Genetics.* 1978; 89: 583–590. PMID: [17248844](https://pubmed.ncbi.nlm.nih.gov/17248844/)

74. Takezaki N, Nei M, Tamura K. POPTREE2: Software for constructing population trees from allele frequency data and computing other population statistics with Windows-interface. *Molecular Biology and Evolution*. 2010; 27:747–752. doi: [10.1093/molbev/msp312](https://doi.org/10.1093/molbev/msp312) PMID: [20022889](https://pubmed.ncbi.nlm.nih.gov/20022889/)
75. Wilson GA, Rannala B. Bayesian inference of recent migration rates using multilocus genotypes. *Genetics*. 2003; 163: 1177–1191. PMID: [12663554](https://pubmed.ncbi.nlm.nih.gov/12663554/)
76. Jost L. GST and its relatives do not measure differentiation. *Molecular Ecology*. 2008; 17(18): 4015–4026. PMID: [19238703](https://pubmed.ncbi.nlm.nih.gov/19238703/)
77. Manni F, Guérard E, Heyer E. Geographic patterns of (genetic, morphologic, linguistic) variation: how barriers can be detected by “Monmonier’s algorithm”. *Human Biology*. 2004; 76: 173–190. PMID: [15359530](https://pubmed.ncbi.nlm.nih.gov/15359530/)
78. Jensen JL, Bohonak AJ, Kelley ST. Isolation by distance, web service. *BMC Genetics*. 2005; 6: 13. v.3.23 <http://ibdws.sdsu.edu/> PMID: [15760479](https://pubmed.ncbi.nlm.nih.gov/15760479/)
79. Hill C, Menemenlis D, Ciotti B, Henze C. Investigating solution convergence in a global ocean model using a 2048-processor cluster of distributed shared memory machines. *Scientific Programming*. 2007; 12: 107–115.
80. Menemenlis D, Campin JM, Heimbach P, Hill C, Lee T, Nguyen A, Schodlok M, Zhang H 2008. ECCO2: High resolution global ocean and sea ice data synthesis. *Mercator Ocean Quarterly Newsletter*, 31:13–21.
81. Smith WHF, Sandwell DT. Global seafloor topography from satellite altimetry and ship depth soundings. *Science*. 1997; 277: 1957–1962
82. Menezes MPM, Berger U, Mehlig U. Mangrove vegetation in Amazonia: a review of studies from the coast of Pará and Maranhao States, north Brazil. *Acta Amazonica*. 2008; 38: 403–420.
83. Menezes MPM, Oliveira D, Mello CF. Pollination of red Mangrove *Rhizophora mangle* in the northern Brazil. *Acta Horticulturae*. 1997; 437: 431–434.
84. Nadia TL, Machado IC. Wind pollination and propagule formation in *Rhizophora mangle* L. (Rhizophoraceae): resource or pollination limitation?. *An Acad Bras Cienc*. 2014; 86: 229–38. PMID: [24804313](https://pubmed.ncbi.nlm.nih.gov/24804313/)
85. Wee K.S. Genetic Connectivity of four mangrove species from the Malay Peninsula. (PhD Thesis). National University of Singapore. 2013: 147pp.
86. Loveless MD, Hamrick JL. Ecological determinants of genetic structure in plant populations. *Ann. Rev. Eco. Syst.* 1984; 15:65–95.
87. Di Nitto D, Neukermans G, Koedam N, Defever H, Pattyn F, Kairo JG, et al. Mangroves facing climate change: landward migration potential in response to projected scenarios of sea level rise. *Biogeosciences*. 2014; 11: 857–871s.
88. Nilsson C, Brown RL, Jansson R, Merritt DM. The role of hydrochory in structuring riparian and wetland vegetation. *Biol Rev Camb Philos Soc*. 2010; 85:837–58. doi: [10.1111/j.1469-185X.2010.00129.x](https://doi.org/10.1111/j.1469-185X.2010.00129.x) PMID: [20233190](https://pubmed.ncbi.nlm.nih.gov/20233190/)
89. Ellison JC, Zouh I. Vulnerability to Climate Change of Mangroves: Assessment from Cameroon, Central Africa. *Biology* 2012; 1: 617–638. doi: [10.3390/biology1030617](https://doi.org/10.3390/biology1030617) PMID: [24832511](https://pubmed.ncbi.nlm.nih.gov/24832511/)
90. Munji CA, Bele MY, Iidinoba ME, Sonwa DJ. Floods and mangrove forests, friends or foes? Perceptions of relationships and risks in Cameroon coastal mangroves. *Estuarine, Coastal and Shelf Science*. 2014; 140: 67–75.
91. Slatkin M. Gene flow and the geographic structure of natural populations. *Science*. 1987; 236: 787–792. PMID: [3576198](https://pubmed.ncbi.nlm.nih.gov/3576198/)
92. Rabinowitz D. Dispersal properties of mangrove propagules. *Biotropica*. 1978; 10: 47–57.
93. Clarke PJ, Kerrigan RA, Westphal CJ. Dispersal potential and early growth in 14 tropical mangroves: do early life history traits correlate with patterns of adult distribution?. *Journal of Ecology*. 2001; 89: 648–659.
94. Drexler J. Maximum longevities of *Rhizophora apiculata* and *R. mucronata*. *Pacific Science*. 2001; 55: 17–22.
95. Allen JA, Krauss KW. The influence of propagule flotation longevity and light availability on the establishment of introduced mangrove species in Hawai'i. *Pacific Science*. 2006; 60: 657–669.
96. Steele O. Natural and anthropogenic biogeography of mangroves in the Southwest Pacific. PhD Dissertation. University of Hawai'i, Manoa. 2006; pp. 93.
97. Wood S, Paris CB, Ridgwell A, Hendy EJ. Modelling dispersal and connectivity of broadcast spawning corals at the global scale. *Global Ecology and Biogeography*. 2014; 23: 1–11.
98. Ternon JF, Roberts MJ, Morris T, Hancke L, Backeberg B. In situ measured current structures of the eddy field in the Mozambique Channel. *Deep-Sea Research II*. 2014; 100: 10–26.

99. Hancke L, Roberts MJ, Ternon JF. Surface drifter trajectories highlight flow pathways in the Mozambique Channel. *Deep-Sea Research II*. 2014; 100: 27–37.
100. Nathan R. The challenges of studying dispersal. *Trends in Ecology & Evolution*. 2001; 16: 481–483.
101. Mitarai S, Siegel DA, Watson JR, Dong C, McWilliams JC. Quantifying connectivity in the coastal ocean with application to the Southern California Bight. *Journal of Geophysical Research*. 2009; 114, C10026, doi: [10.1029/2008JC005166](https://doi.org/10.1029/2008JC005166)
102. Watson J, Mitarai S, Siegel D, Caselle J, Dong C, McWilliams J. Realized and potential larval connectivity in the Southern California Bight. *Marine Ecology Progress Series*. 2010; 401: 31–48.
103. White C, Selkoe KA, Watson J, Siegel DA, Zacherl DC, Toonen RJ. Ocean currents help explain population genetic structure. *Proceedings of the Royal Society B: Biological Sciences*. 2010; 277: 1685–1694. doi: [10.1098/rspb.2009.2214](https://doi.org/10.1098/rspb.2009.2214) PMID: [20133354](https://pubmed.ncbi.nlm.nih.gov/20133354/)
104. Simpson S, Harrison HB, Claereboudt MR, Planes S. Long-distance dispersal via ocean currents connects Omani clownfish populations throughout entire species range. *PLoS ONE*. 2014; 9: e107610. doi: [10.1371/journal.pone.0107610](https://doi.org/10.1371/journal.pone.0107610) PMID: [25229550](https://pubmed.ncbi.nlm.nih.gov/25229550/)
105. Steinke TD, Ward CJ. Use of plastic drift cards as indicators of possible dispersal of propagules of the mangrove *Avicennia marina* by ocean currents. *African Journal of Marine Science*. 2003; 25: 169–176.
106. Frankham R. Relationship of genetic variation to population size in wildlife. *Conservation Biology*. 1996; 10: 1500–1508.
107. Lammi A, Siikmäki P, Mustajärvi K. Genetic diversity, population size, and fitness in central and peripheral populations of a rare plant *Lychnis viscaria*. *Conservation Biology*. 1999, 13: 1069–1078.
108. Alemagi D, Oben PM, Ertel J. Mitigating Industrial Pollution along the Atlantic Coast of Cameroon: An Overview of Government Efforts. *Environmentalist*. 2006; 26:41–50.
109. Ngeve MN, Leermakers M, Elskens M, Kochzius M. Assessment of trace metal pollution in sediments and intertidal fauna at the coast of Cameroon. *Environ Monit Assess*. 2015c; 187:337. doi: [10.1007/s10661-015-4574-7](https://doi.org/10.1007/s10661-015-4574-7)
110. Ng LW, Onishi Y, Inomata N, Teshima KM, Chan HT, Baba S, et al. Closely related and sympatric but not all the same: genetic variation of Indo-West Pacific *Rhizophora* mangroves across the Malay Peninsula. *Conserv Genet*. 2015; 16:137–150. doi: [10.1007/s10592-014-0647-3](https://doi.org/10.1007/s10592-014-0647-3)
111. Wee AKS, Takayama K, Chua JL, Asakawa T, Meenakshisundaram SH, Onrizal, et al. Genetic differentiation and phylogeography of partially sympatric species complex *Rhizophora mucronata* Lam. and *R. stylosa* Griff. using SSR markers. *BMC Evolutionary Biology*. 2015; 15:57 doi: [10.1186/s12862-015-0331-3](https://doi.org/10.1186/s12862-015-0331-3) PMID: [25888261](https://pubmed.ncbi.nlm.nih.gov/25888261/)
112. Dakin EE, Avise JC. Microsatellite null alleles in parentage analysis. *Heredity*. 2004; 93, 504–509. PMID: [15292911](https://pubmed.ncbi.nlm.nih.gov/15292911/)
113. Van Oosterhout C, Weetman D, Hutchinson WF. Estimation and adjustment of microsatellite null alleles in nonequilibrium populations. *Mol Ecol Notes*. 2006; 6:255–256.
114. De Ryck DJR, Robert EMR, Schmitz N, Van der Stocken T, Di Nitto D, Dahdouh-Guebas et al. Size does matter, but not only size: two alternative dispersal strategies for viviparous mangrove propagules. *Aquat. Bot*. 2012; 103:66–73.
115. Britton JC, Morton B. *Shore Ecology of the Gulf of Mexico*. University of Texas Press; 1st Ed. May 1, 1989. ISBN-13: 978-0292776265.
116. Schupp EW, Jordano P, Gomez JM. Seed dispersal effectiveness revisited: a conceptual review. *New Phytologist*. 2010; 188: 333–353. doi: [10.1111/j.1469-8137.2010.03402.x](https://doi.org/10.1111/j.1469-8137.2010.03402.x) PMID: [20673283](https://pubmed.ncbi.nlm.nih.gov/20673283/)